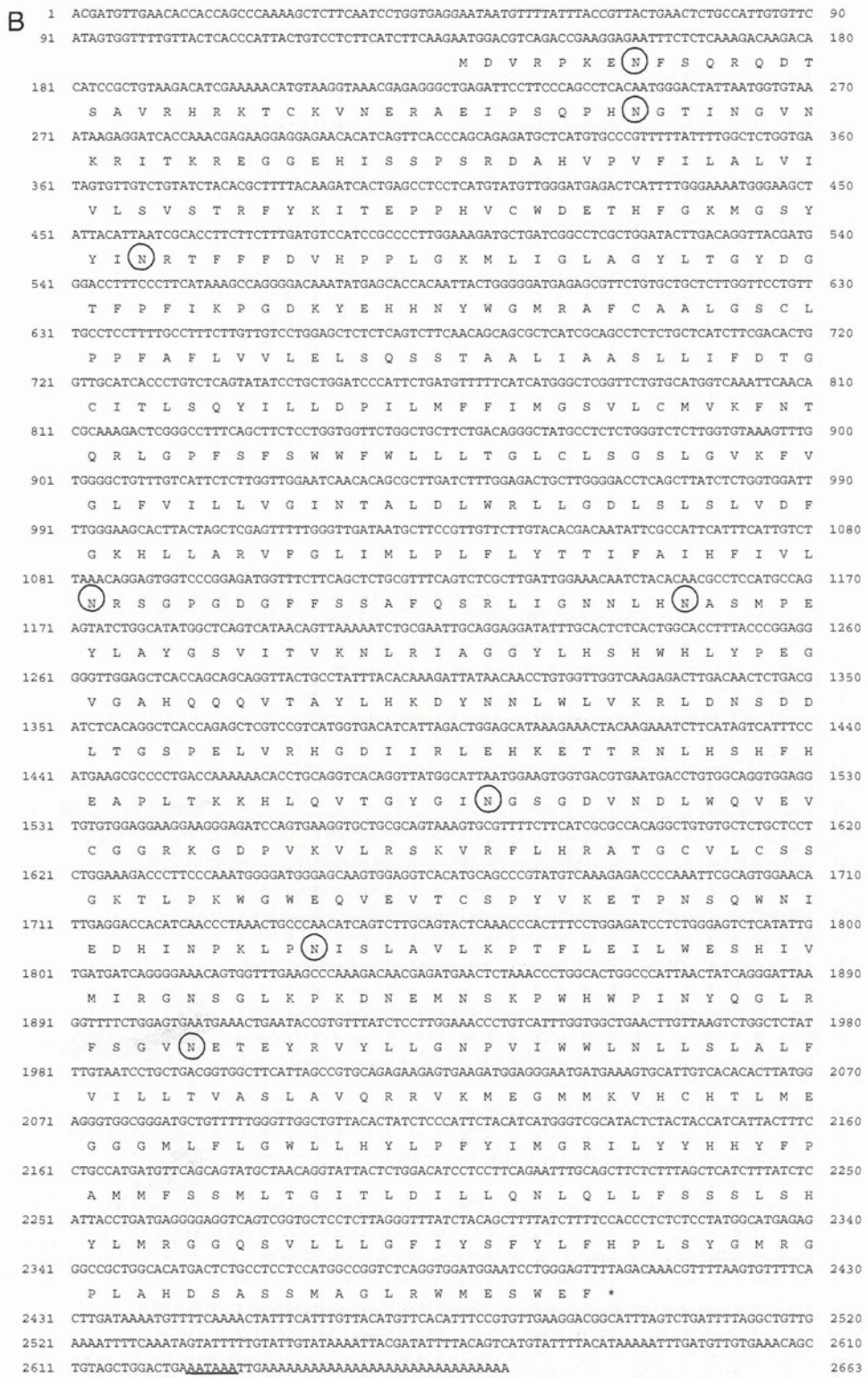

Fig. 1. Nucleotide sequences and deduced amino acid sequences of *zPOMT1* and *zPOMT2*. The cDNA sequences of zebrafish *POMT1* (**A**) and *POMT2* (**B**) genes are presented on the upper line. Deduced amino acid sequences are indicated by the single-letter amino acid codes. Potential *N*-glycosylation sites are indicated by circles. Consensus polyadenylation sites are underlined.

neuronal migration and eye anomalies (Beltran-Valero de Bernabe et al. 2002; van Reeuwijk et al. 2005). POMT orthologs have been identified in many animals, including *Drosophila* (Martín-Blanco and García-Bellido 1996; Willer et al. 2002), mouse (Willer et al. 2002; Willer et al. 2004), rat (Manya et al. 2006) and humans (Jurado et al. 1999; Willer et al. 2002). *Drosophila*, rat and mouse have orthologs of both of human *POMT* genes, and their products have protein *O*-mannosyltransferase activity when only they are co-expressed (Ichimiya et al. 2004; Manya et al. 2006; Lommel et al. 2008). In contrast, *Drosophila* does not have orthologs to human or murine protein *O*-mannose β1,2-*N*-acetylglucosaminyltransferase1 (POMGnT1) (Ichimiya et al. 2004). POMGnT1 catalyzes the transfer of GlcNAc from UDP-GlcNAc to the protein *O*-mannosyl residue (Yoshida et al. 2001; Liu et al. 2006; Miyagoe-Suzuki et al. 2009). Therefore, it seems that the structures of *O*-mannosylglycans of invertebrates are quite different from those of vertebrates. Moreover, it has been reported that hPOMT1 and hPOMT2 must form a heterocomplex for protein *O*-mannosyltransferase activity (Akasaka-Manya et al. 2006).

The zebrafish (*Danio rerio*) provides a readily accessible model for human muscle diseases such as muscular dystrophies (Bassett and Currie 2003). Muscle specification and differentiation follow a well-characterized time course and allow detailed analysis with single-cell resolution (Devoto et al. 1996). Zebrafish orthologs of proteins in the human DGC have been implicated in muscle development, and some zebrafish DGC orthologs have uses as models to study human muscular dystrophy and congenital myopathy (Parsons et al. 2002; Bassett and Currie 2003; Guyon et al. 2003). More recently, it has been reported that the zebrafish has orthologs of *POMT1*, *POMT2*, *POMGnT1* and other putative glycosyltransferases expected to contribute to the synthesis of mammalian-type *O*-mannosylglycan (Steffen et al. 2007; Moore et al. 2008). Taken together, the structures of *O*-mannosylglycans are thought to be similar in diverse vertebrates. Therefore, zebrafish may be a useful model for analyses of the biosynthetic

A

```
hPOMT1   1:----------------------MWGFLKRPVVVTADINLSLVALTGMGLLSRLWRLTYPRAVVFDEVYYGQYISFYMKQIFFLDDSGPPF 68
mPOMT1   1:MGSHSTGLEETLGVLPSWLFCKMLRFLKRPLVVTVDINLNLVALTGLGLLTRLWQLSYPRAVVFDEVYYGQYISFYMKRIFFLDDSGPPF 90
rPOMT1   1:MGNRSMGREDTLGVLPSLLFCKMLRFLKRPLVVTIDINLNLVALTVLGLLTRLWQLSYPRAVVFDEVYYGQYISFYMKRVFFLDDSGPPF 90
zPOMT1   1:----------------------MQ-CVKLPVSVTVEINVLLLAVTALALFTRLYGIHFPKAVVFDEVYYGQFLSLYMKQVFFIDESGPPF 67

hPOMT1  69:GHMVLALGGYLGGFDGNFLWNRIGAEYSSNVPVWSLRLLPALAGALSVPMAYQIVLELHFSHCAAMGAALLMLIENALITQSRLMLLESV 158
mPOMT1  91:GHMLLALGGWLGGFDGNFLWNRIGAEYSSNVPIWSLRLLPALAGALSVPMAYQIVLELHFSHGAAIGAALLMLIENALITQSRLMLLESI 180
rPOMT1  91:GHMLLALGGWLGGFDGNFLWNRIGAEYSSNVPVWSLRLLPALAGALSVPMAYQIVLELHFSHCTAMGAALLMLIENALITQSRLMLLESI 180
zPOMT1  68:GHMILALGAYLGGFDGNFVWNRIGAEYPGNVPVWSLRLIPALAGSFCVPLAYLVVVELGYSHFSALGACALLLMENSLIVQSRFMLLESV 157

hPOMT1 159:LIFFNLLAVLSYLKFFNCQKHSPFSLSWWFWLTLTGVACSCAVGIKYMGVFTYVLVLGVAAVHAWHLLGDQTLSNVCVFCHLLARAVALL 248
mPOMT1 181:LIFFNLLAVLSYLKFFNSQTHSPFSVHWWLWLLLTGVSCSCAVGIKYMGIFTYLLVLGIAAVHAWNLIGDQTLSNMRVLSHLLARIVALL 270
rPOMT1 181:LIFFNLLAVLSYLKFFNSQTHSPFSVHWWLWLMLTGVSCSCAVGIKYMGIFTYLLVLSIAAVHAWHLIGDQTLSNICVLSHLLARAVALL 270
zPOMT1 158:LIFFLLLAVLSYLRFHKARN----SFFKWFWLVICGVSCAFGIGVKYMGMFTYFLLLSLAAVHTWQLIGDRTLSHGKVMFQVLVRFLALV 243

hPOMT1 249:VIPVVLYLLFFYVHLILVERSGPHDQIMSSAFQASLEGGLARITQGQPLEVAFGSQVTLRNVFGKPVPCWLHSHQDTYPMIYENGRGSSH 338
mPOMT1 271:VVPVFLYLLFFYVHLMLLYRSGPHDQIMSSAFQASLEGGLARITQGQPLEVAFGSQVTLKSVSGKPLPCWLHSHKNTYPMIYENGRGSSH 360
rPOMT1 271:VVPVFLYLLFFYVHLMLLYRSGPHDQIMSSAFQASLEGGLARITQGQPLEVAFGSQVTLKSVSGKPLPCWLHSHKNTYPMIYENGRGSSH 360
zPOMT1 244:VLPVIIYLGFFYIHLTLLYRSGPSDQMMSSAFQASLEGGLARITQGQPLDVAFGSQVTLRTVSGKPVPCWLHSHKANYPIRYENGRGSSH 333

hPOMT1 339:QQQVTCYPFKDVNNWWIVKDPRRHQLVVSSPPRPVRHGDMVQLVHGMTTRSLNTHDVAAPLSPHSQEVSCYIDYNISMPAQNLWRLEIVN 428
mPOMT1 361:QQQVTCYPFKDINNWWIVKDPGRHQLVVNNPPRPVRHGDIVQLVHGMTTRLLNTHDVAAPLSPHSQEVSCYIDYNISMPAQNLWKLDIVN 450
rPOMT1 361:QQQVTCYPFKDINNWWIVKDPGRHQLVVNNPPRPVRHGDIVQLVHGMTTRLLNTHDVAAPLSPHSQEVSCYIDYNISMPAQNLWKLDIVN 450
zPOMT1 334:QQQVTCYPFKDVNNWWIIKDPGRQSLVVSSPPRPVRHGDIIQLLHGMTTRYLNTHDVAAPMSPHSQEVSGYIDFNVSMPAQNLWRVDIVN 423

hPOMT1 429:RGSDTDVWKTILSEVRFVHVNTSAVLKLSGAHLPDWGYRQLEIVGEKLSRGYHGSTVWNVEEHRYGASQEQRERERELHSPAQVDVSRNL 518
mPOMT1 451:RESNRDIWKTILSEVRFVHVNTSAILKLSGAHLPDWGFRQLEVVGEKLSPGYHPSMVWNVEEHRYGKSHEQKERELELHSPTQLDISRNL 540
rPOMT1 451:RESNQDIWKTILSEVRFVHVNTSAILKLSGAHLPDWGFRQLEVVGEKLSLGPHPSMVWNVEEHRYGRGHEQKERELELHSPTQHDISRNL 540
zPOMT1 424:RESEKEIWKTILSEVRLVHVNTSAVLKLSGASLPEWGFKQLEVVGDKIYKGYQQTGMWNVEEHRYGRSQEPKERELELKSPTHSDVNKNL 513

hPOMT1 519:SFMARFSELQWRMLALRSDDSEHKYSSSPLEWVTLDTNIAYWLHPRTSAQIHLLGNIVIWVSGSLALAIYALLSLWYLLRRRRNVHDLPQ 608
mPOMT1 541:SFMARFSELQWKMLTLKNEDLEHQYSSTPLEWLTLDTNIAYWLHPRTSAQIHLLGNIVIWTSASLATVVYTLLFFWYLLRRRRSICDLPE 630
rPOMT1 541:SFMARFSELQWKMLTLKNEDLEHQYSSTPLEWLTLDTNIAYWLHPRTSAQIHLLGNIVIWTSASLATVAYTLLFFWYLLRRRRNICDLPE 630
zPOMT1 514:TFMAKFLELQWKMLTVKNEESEHKYSSSPLEWITMDTNIAYWLHPSSNAQIHFIGNIVTWTTGNITLVVYCLLFLTYLLRRRRKVEDIPQ 603

hPOMT1 609:DAWLRWVLAGALCAGGWAVNYLPFFLMEKTLFLYHYLPALTFQILLLPVVLQHISDHLCRSQLQRSIFSALVVAWYSSACHVSNTLRPLT 698
mPOMT1 631:DAWSRWVLAGALCTGGWAINYLPFFLMERVLFLYHYLPALTFQILLLPIVLQHASDHLCRSQLQRNVFSALVVAWYSSACHVSNMLRPLT 720
rPOMT1 631:DAWSHWVLAGALCIGGWAINYLPFFLMERMLFLYHYLPALTFQILLLPIVMQHASDHLCRSQLQRNVFSALVVAWYSSACHVSNMLRPLT 720
zPOMT1 604:DSWEQLALAGVVCFGGWAVNYLPFFLMEKTLFLYHYLPALTFKILQIPIVTEHLYIHVLRSSAQQKAFGGVILAVLCSVYMSYHSLSPLT 693

hPOMT1 699:YGDKSLSPHELKALRWKDSWDILIRKH                                                              725
mPOMT1 721:YGDTSLSPGELRALRWKDSWDILIRK                                                               746
rPOMT1 721:YGDTSLSPGELRALRWKDSWDILIRKY                                                              747
zPOMT1 694:YGQPALTSDKFAELRWRESWDILLRKR                                                              720
```

B

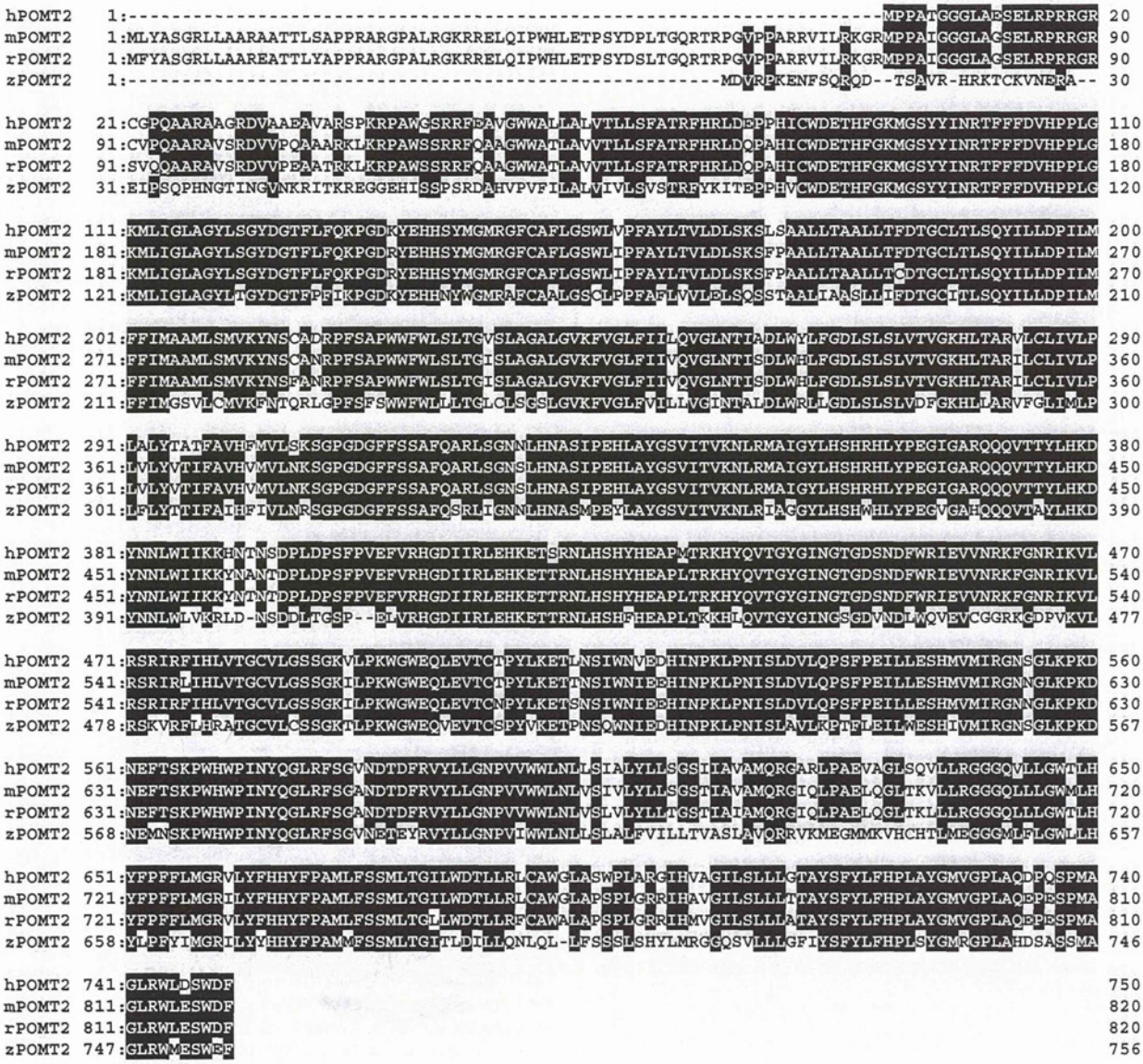

pathway of *O*-mannosylglycans in vertebrates, the mechanisms of muscular dystrophies, and myogenesis.

In this study, we isolated and cloned full-length cDNAs encoding two zebrafish *POMT* genes, *zPOMT1* and *zPOMT2*, and examined whether they have protein *O*-mannosyltransferase activity. We also investigated the expression patterns of both genes during embryogenesis and in adult tissues. Furthermore, we analyzed the distribution and localization of a protein expressed from constructs containing the 3′untranslated region (3′UTR) of *zPOMT1* or *zPOMT2*. Finally, knockdown analysis using antisense morpholino oligonucleotides (MOs) was performed to assess the function of protein *O*-mannosylation during zebrafish development.

Results

cDNA cloning and sequencing of zPOMT1 and zPOMT2

The full-length cDNAs encoding *zPOMT1* and *zPOMT2* genes were cloned by reverse transcriptase-polymerase chain reaction (RT-PCR) using zebrafish embryos. The complete cDNAs and deduced amino acid sequences of *zPOMT1* and *zPOMT2* are shown in Figure 1 (GenBank accession nos. AB281275 and AB281276, respectively). *zPOMT1* consisted of an open reading frame (ORF) of 2160 bases encoding a conceptual translation product of 720 amino acids with a predicted molecular mass of 82,036 Da (Figure 1A). *zPOMT2* consisted of an ORF of 2268 bases encoding conceptual translation product of 756 residues with a predicted molecular mass of 85,710 Da

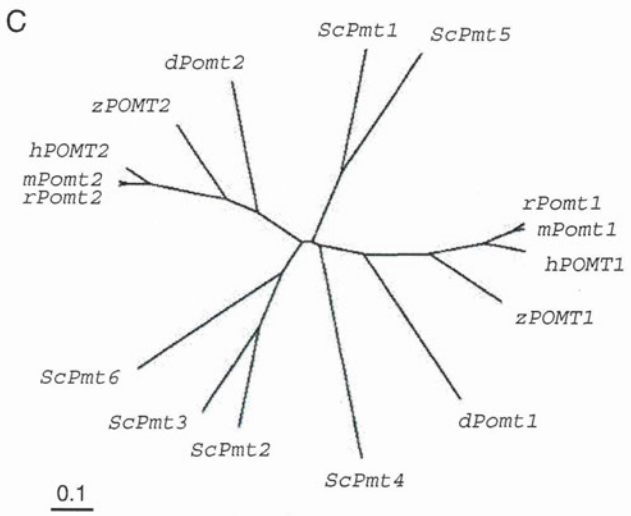

Fig. 2. Comparisons of human, mouse, rat and zebrafish POMTs. ClustalW alignments of human (h), mouse (m), rat (r) and zebrafish (z) POMT1 (**A**) and POMT2 (**B**) amino acid sequences are indicated by single-letter amino acid codes, respectively. Conserved amino acids are highlighted. (**C**) ClustalW phylogenic tree of human, mouse, rat, zebrafish and *Drosophila* (d) POMTs and *S. cerevisiae* (Sc) Pmts. The amino acid sequence of hPOMT1 is a major type that was used for assay of protein *O*-mannosyltransferase activity in this study. The amino acid sequences of mPOMT2 and rPOMT2 belonged to the testis form. The branch lengths indicate amino acid substitutions per site.

(Figure 1B). A consensus polyadenylation site (AATAAA) was located downstream of the translation termination codon in both *zPOMT1* and *zPOMT2*. As shown in Figure 2, the deduced amino acid sequences in both zPOMT1 and zPOMT2 were similar to those of mammals such as human, mouse and rat (Jurado et al. 1999; Willer et al. 2002; Willer et al. 2004; Manya et al. 2006). zPOMT1 had 66% identity to hPOMT1 (Figure 2A), whereas zPOMT2 showed 70% identity to hPOMT2 (Figure 2B). A phylogenetic analysis of 16 proteins—six *Saccharomyces cerevisiae* Pmts (ScPmt1-6) (Willer et al. 2002), two human (hPOMT1 and hPOMT2), two mouse (mPOMT1 and mPOMT2), two rat (rPOMT1 and rPOMT2), two *Drosophila* (dPOMT1 and dPOMT2) and two zebrafish (zPOMT1 and zPOMT2)—indicates that zPOMT1 is in the pmt4 subfamily and zPOMT2 is in the pmt2 subfamily (Figure 2C).

Gene expression of zPOMT1 and zPOMT2

Quantitative PCR was performed with early developmental stages (Figure 3A) and all adult tissues (Figure 3B). There were significant differences in the levels of *zPOMT1* and *zPOMT2* expression during embryogenesis. At 0 h post fertilization (hpf), both genes, *zPOMT1* and *zPOMT2*, were highly expressed. While *zPOMT1* expression decreased after 6 hpf, *zPOMT2* expression increased at 6 hpf and then decreased at 12 hpf. Furthermore, *zPOMT2* expression increased again around 24 hpf. There were no significant differences in *zPOMT1* and *zPOMT2* expression levels in males and females in any adult tissue except for the liver. Interestingly, *zPOMT1* and *zPOMT2* were highly expressed in both testis and ovary (Figure 3B). By means of whole-mount in situ hybridization, mRNAs of *zPOMT1* and *zPOMT2* were detected during early developmental stages. Both *zPOMT1* (Figure 3C) and *zPOMT2* (Figure 3D) transcripts were ubiquitously expressed throughout the gastrulation, tailbud and somite stages. At 24 hpf, both *zPOMT1* and *zPOMT2* mRNAs were detected predominantly in eyes and somites.

Localization of 3′UTRs in zPOMT1 and zPOMT2

The 3′UTR of an mRNA can affect the expression and/or localization of the mRNA during development within particular cells, including primary germ cells (Hashimoto et al. 2009). Therefore, to investigate the function of 3′ UTRs of *zPOMT1* and *zPOMT2*, we fused the 3′UTR of each *zPOMT* to the *enhanced green fluorescent protein* (*EGFP*) gene (Figure 3E). Capped mRNAs of *EGFP*-3′UTR of *zPOMT1* and *zPOMT2* were synthesized and injected into embryos at the one- to two-cell stage. With both constructs, EGFP was distributed throughout the whole body at 6 hpf, and EGFP was highly expressed in the eye, hindbrain and somite from 18 to 24 hpf (Figure 3F).

Knockdown analysis of zPOMT1 and zPOMT2

Antisense MOs against *zPOMT1* and *zPOMT2* were injected into the zebrafish embryos at the one- to two-cell stage, and the developmental progress of the morphants was compared with that of uninjected and control MO embryos (Figure 4). There were no significant differences between control MO and morphant embryos until 12 hpf. At 18 hpf, both *zPOMT1* MO and *zPOMT2* MO embryos were developmentally delayed in comparison with control MO (Figure 4A) and uninjected (data not shown) embryos. At 48 and 72 hpf, *zPOMT1* morphants showed slightly curved tails and curvature of the somite boundaries. In contrast, *zPOMT2* morphants at the same stage showed more severe phenotypes—including twisted tails, aberrant pericardium and abnormal eye pigmentation—than did the *zPOMT1* morphants. Quantitative analyses of embryos from all treatment groups were performed at 96 hpf. Each

Fig. 3. Gene expressions and whole-mount in situ hybridization for *zPOMT1* and *zPOMT2*. Quantitative PCR analyses of *zPOMT1* and *zPOMT2* mRNAs during early developmental stages (**A**) and in adult tissues (**B**). PCR products of *zPOMT1* and *zPOMT2* were detected throughout early developmental stages and in all tissues predominantly in gonads. *zβ-actin2* and *zCox1* were used as internal controls for quantitative PCR in early developmental stages and adult tissues, respectively. B, brain; E, eye; H, heart ; M, muscle ; T, testis; O, ovary; LM, liver (male); LF, liver (female); IM, intestine (male); IF, intestine (female); KM, kidney (male); KF, kidney (female); SM, spleen (male); SF, spleen (female). All reactions were performed in triplicate, and average values ± SD are shown. *zPOMT1* (**C**) and *zPOMT2* (**D**) mRNAs were detected. Both genes were expressed ubiquitously throughout early developmental stage, and high levels of expression were detected at 24 hpf. Arrowheads and boxes shown in the right columns at 24 hpf indicate eyes and the central parts of the somites, respectively. Boxes in 24 hpf were enlarged and shown in the far right panels. Scale bars = 100 μm. Illustration of capped mRNA structure (**E**) and localization of *EGFP*-3′UTR of control (upper panel), *zPOMT1* (middle panel) and *zPOMT2* (lower panel) (**F**). Arrows and arrowheads indicate the proteins corresponding to EGFP-*zPOMTs* 3′UTR. At 24 hpf, EGFP-3′UTR of *zPOMT1* was located predominately to the eye (arrowhead), whereas EGFP-3′UTR of *zPOMT2* was expressed highly in eye (arrowhead), hindbrain (arrow), and somite (bracket). Scale bars = 100 μm.

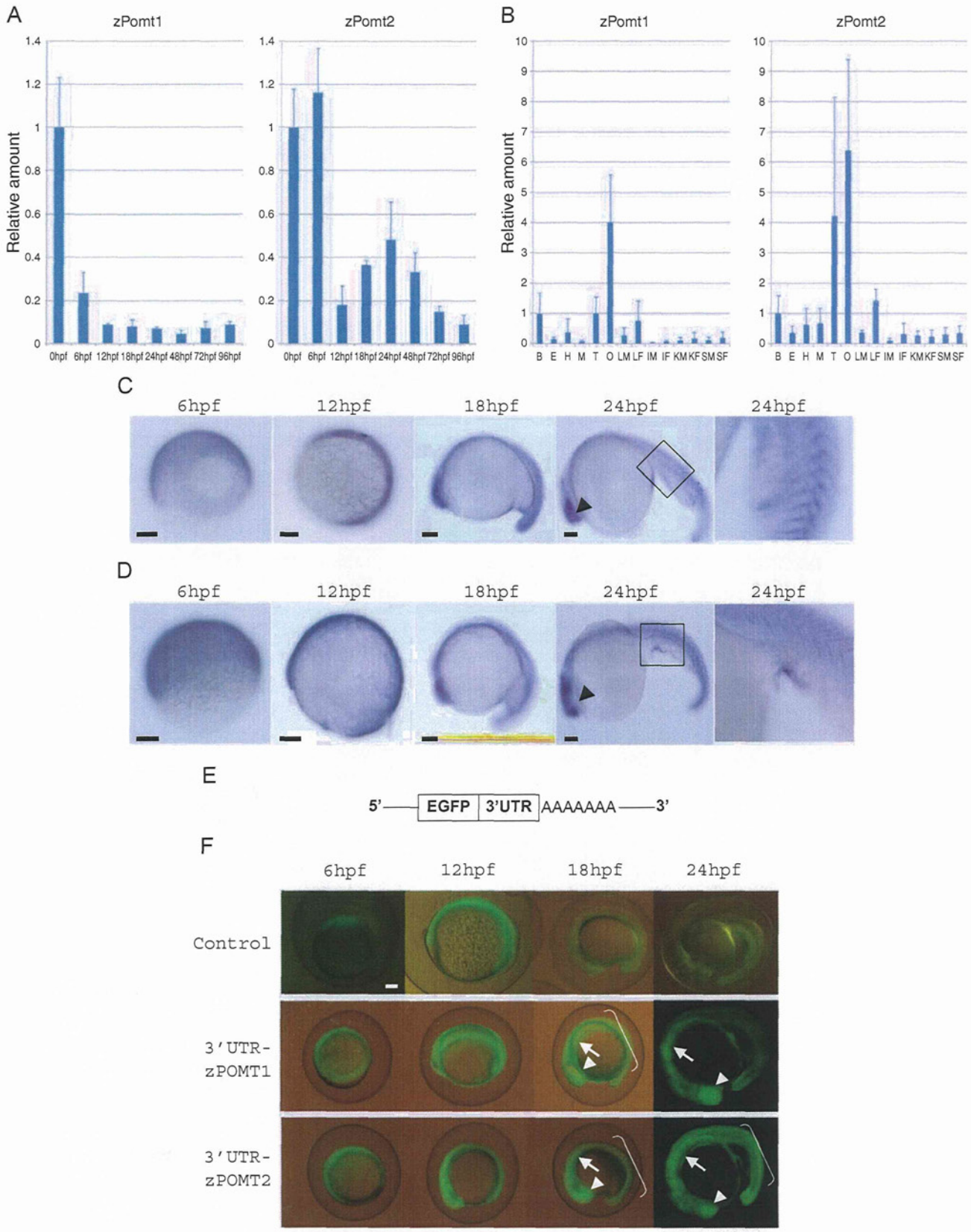
A
zPomt1
zPomt2
Relative amount
0hpf 6hpf 12hpf 18hpf 24hpf 48hpf 72hpf 96hpf
B
zPomt1
zPomt2
Relative amount
B E H M T O LM LF IM IF KM KF SM SF
C
6hpf
12hpf
18hpf
24hpf
24hpf
D
6hpf
12hpf
18hpf
24hpf
24hpf
E
5'
EGFP
3'UTR
AAAAAAA
3'
F
6hpf
12hpf
18hpf
24hpf
Control
3'UTR-zPOMT1
3'UTR-zPOMT2

embryo with or without MO treatment was categorized as having normal, moderate or severe phenotypes according to morphological characteristics (Table I). The frequency of moderate and severe phenotypes increased with injection of increasing amounts of *zPOMT1* and *zPOMT2* MOs. The *zPOMT2* MO embryos had more severe deformities than did the *zPOMT1* MO embryos (Figure 4B, Table I). For example, aberrant eye pigmentation was observed only in *zPOMT2* MO embryos. Finally, swim bladders were not completely formed in *zPOMT1* and *zPOMT2* morphant embryos in comparison with uninjected or control MO embryos (Figure 4B).

To investigate the glycosylation status of α-DG in *zPOMT1* and *zPOMT2* morphant embryos, we immunostained embryos at 48 hpf with the anti-glycosylated α-DG antibody IIH6 (Figure 4C). Strong signals were detected with IIH6 in untreated embryos. Moreover, IIH6 reactivity in control MO embryos was also detected in the horizontal and vertical myosepta. However, the reactivity was almost completely lost in *zPOMT1* and *zPOMT2* morphants.

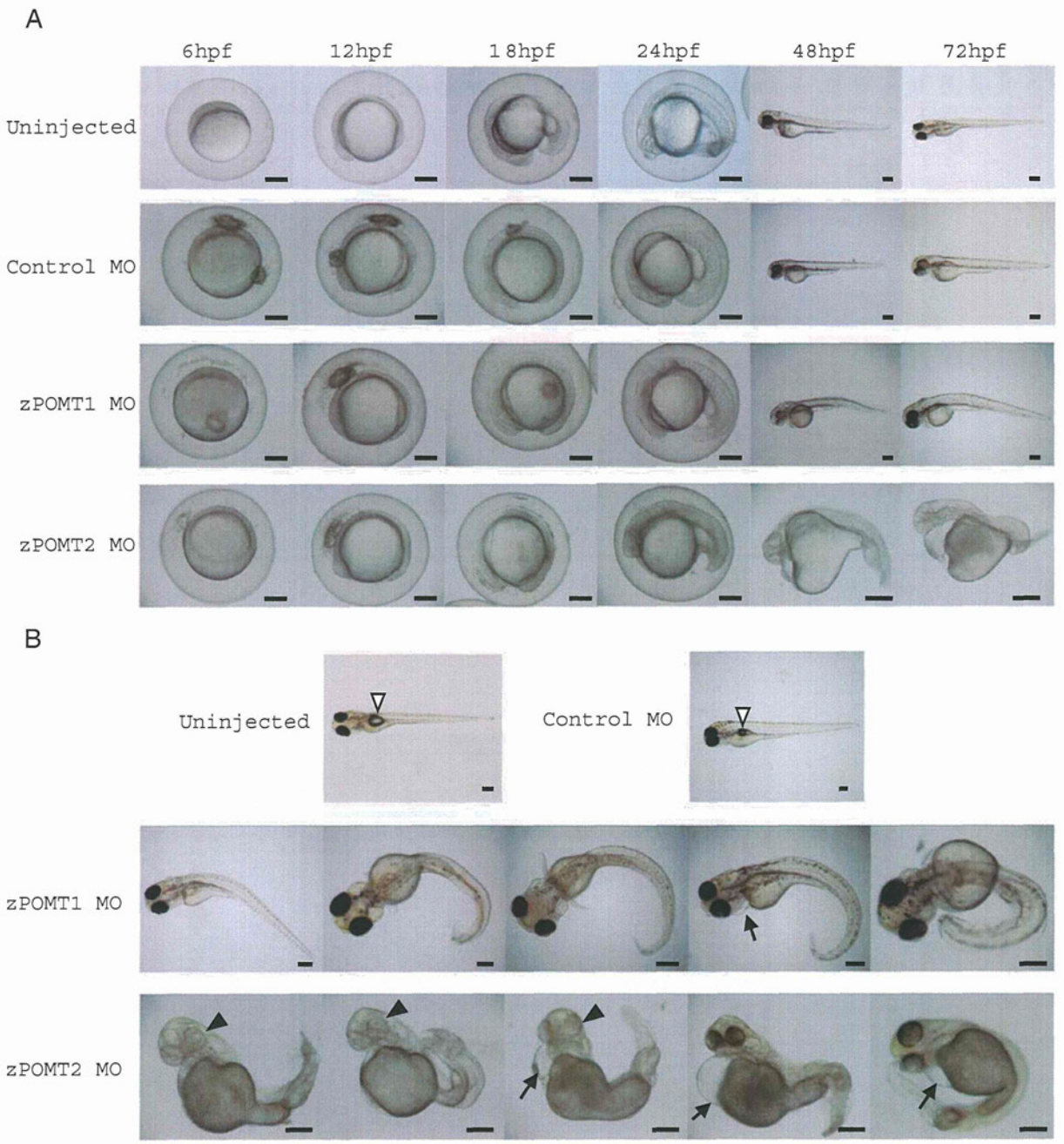

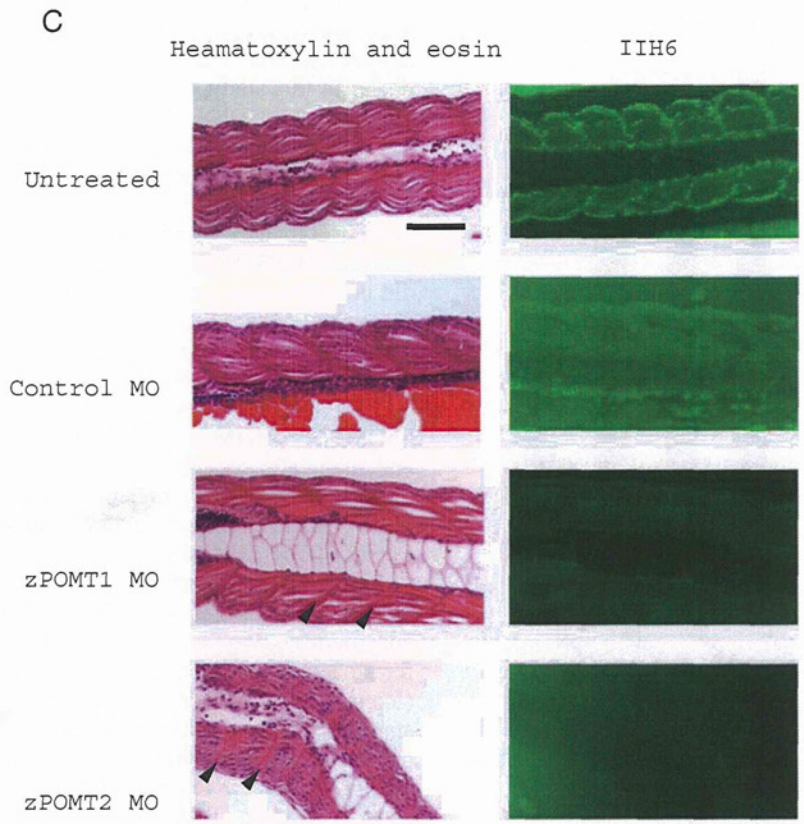

Fig. 4. Knockdown analysis of *zPOMT1* and *zPOMT2*. (**A**) Sequential changes during early developmental stages (6–72 hpf) of uninjected embryos (top panel), embryos injected with control MO (middle upper panel), embryos injected with *zPOMT1* MO (middle lower panel) and embryos injected with *zPOMT2* MO (bottom panel). Zebrafish embryos were injected with each MO at the one- to two-cell stage and were observed at 6, 12, 18, 24, 48 and 72 hpf. Scale bars = 200 μm. (**B**) 96 hpf morphants. Top panel: uninjected embryo (left side) and injected control MO (right side), embryos injected *zPOMT1* MO (middle panel), and embryos injected *zPOMT2* MO (bottom panel). Zebrafish embryos were injected with each MO at the one- to two-cell stages and were observed at 96 hpf. White arrowheads indicate swim bladder. Both morphant embryos revealed curved tail, and some had abnormal pericardium (arrows). Some of the *zPOMT2* morphants showed aberrant eye pigmentation (arrowheads). Scale bars = 200 μm. (**C**) Whole-mount immunohistochemistry with anti-glycosylated α-DG antibody IIH6 in 48-hpf embryos. Left panels, hematoxylin and eosin staining; right panels, IIH6 staining. IIH6 immunoreactivity was detected in uninjected and control MO but decreased in *zPOMT1* and *zPOMT2* morphants. Arrowheads represent vertical myosepta. Scale bars = 50 μm.

Protein O-mannosyltransferase activity of zPOMT1 and zPOMT2

To analyze the protein *O*-mannosyltransferase activity of zPOMT1 and zPOMT2, the cDNAs were cloned into an expression vector. The resulting expression constructs were transfected into human embryonic kidney 293T (HEK293T) cells, and microsomal membranes were used for enzyme assay. High levels of protein *O*-mannosyltransferase activity was observed only when the *zPOMT1* and *zPOMT2* genes were co-expressed in HEK293T cells (Figure 5). Jack bean α-mannosidase digestion showed that the mannosyl residue was linked to GST-α-DG by α-linkage (data not shown), as reported previously (Manya et al. 2004). Although a single transfection of *zPOMT1* in HEK293T cells did not show any enzymatic activity, transfection of *zPOMT2* alone did result in low levels of activity. Cells co-transfected with *zPOMT1* and *hPOMT2* and cells co-transfected with *hPOMT1* and *zPOMT2* showed robust levels of *O*-mannosyltransferase activity. In contrast, cells co-transfected with *zPOMT1* and *hPOMT1* and cells co-transfected with *zPOMT2* and *hPOMT2* did not show any enzymatic activity (data not shown). These results indicated that POMT1 and POMT2 from zebrafish and humans are interchangeable and that POMT1 and POMT2 have different functional roles in POMT enzymatic activity.

Table I. Quantification of *zPOMT* morphant phenotypes at 96 hpf

	Concentration (mM)	Normal	Moderate	Severe
Uninjected	-	97 (100.0%)	0 (0%)	0 (0%)
Control MO	1.0	65 (95.6%)	3 (4.4%)	0 (0%)
zPOMT1 MO	1.0	65 (79.3%)	14 (17.1%)	3 (3.6%)
	0.5	72 (93.5%)	4 (5.2%)	1 (1.3%)
	0.25	72 (98.6%)	0 (0%)	1 (1.4%)
zPOMT2 MO	1.0	33 (35.5%)	31 (33.3%)	29 (31.2%)
	0.5	55 (61.1%)	26 (28.9%)	9 (10.0%)
	0.25	79 (86.8%)	5 (5.5%)	7 (7.7%)

The phenotypic data shown were obtained from three independent experiments. The number of embryos observed for each phenotypic class is shown and also presented as a percentage of the total number of embryos studied for each morpholino (MO). Moderate (curved tails and curvature of the somite boundaries); Severe (twisted tail and aberrant pericardium).

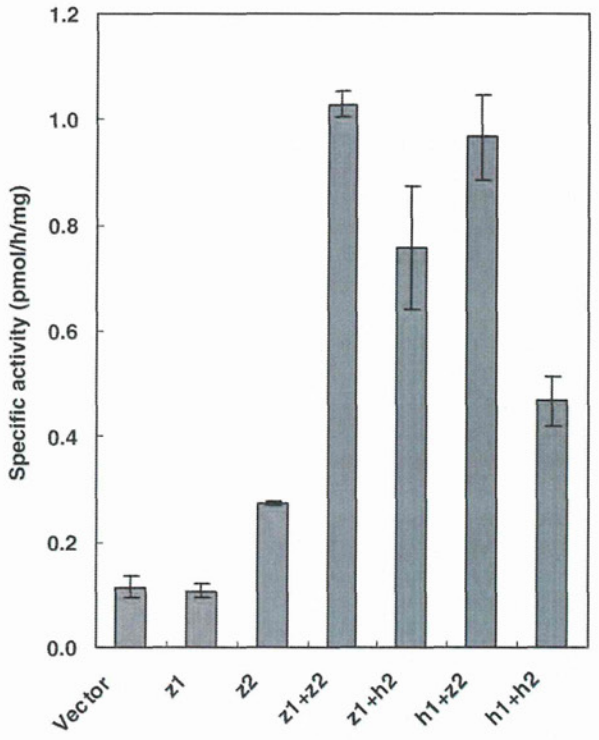

Fig. 5. Protein *O*-mannosyltransferase activities of *zPOMTs*. Protein *O*-mannosyltransferase activity was based on the rate of mannose transfer from mannosylphosphoryldolichol to a GST-α-DG. Vector, cells transfected with vector only; z1, cells transfected with *zPOMT1*; z2, cells transfected with *zPOMT2*; z1+z2, cells co-transfected with *zPOMT1* and *zPOMT2*; z1+h2, cells co-transfected with *zPOMT1* and *hPOMT2*; h1+z2, cells co-transfected with hPOMT1 and *zPOMT2*; h1+h2, cells co-transfected with *hPOMT1* and *hPOMT2*. Average values ± SD of three independent experiments are shown.

Discussion

Zebrafish have been useful for the study of human muscular dystrophies and congenital myopathies (Parsons et al. 2002; Bassett and Currie 2003; Bassett et al. 2003; Guyon et al. 2003) because zebrafish have orthologs of genes implicated in human muscular dystrophies, including *POMT1*, *POMT2*, *POMGnT1*, *dystrophin*, *fukutin* and fukutin-related protein (*FKRP*) (Steffen et al. 2007; Moore et al. 2008). Recently, it has been reported that knockdown analysis of *FKRP*, one of the causative genes in α-dystroglycanopathies, resulted in morphants that showed a pathological spectrum similar to those of human muscular dystrophies associated with mutations in *FKRP* (Thornhill et al. 2008). However, the function of FKRP is not clear yet (Esapa et al. 2002; Esapa et al. 2005; Matsumoto et al. 2004; Dolatshad et al. 2005; Torelli et al. 2005; Beedle et al. 2007). In contrast, POMTs are known to be protein *O*-mannosyltransferases. *FKRP* MO and *zPOMTs* morphant embryos showed a reduction in the glycosylated α-DG staining, indicating that FKRP may affect the biosynthetic pathway of *O*-mannosylglycans (Thornhill et al. 2008).

In mammals, two protein *O*-mannosyltransferase (POMTs) family members, POMT1 and POMT2, are known to exist. hPOMT1 and hPOMT2 catalyze protein *O*-mannosyl transfer to α-DG, which serves as a protein substrate, and mutations in the *hPOMT1* and *hPOMT2* genes result in WWS, a severe muscular dystrophy that also results in structural alterations in eyes and brain malformations, such as cobblestone lissencephaly. In this study, we have identified, cloned and expressed the full-length cDNAs of the *zPOMT1* and *zPOMT2* genes, and our results suggest that high levels of protein *O*-mannosyltransferase activity depends on expression of both genes. Co-expression of both *zPOMT1* and *zPOMT2* genes showed high protein *O*-mannosyltransferase activity similar to results from analyses of hPOMTs. Although transfection of *zPOMT1* alone did not show any enzymatic activity, transfection of *zPOMT2* alone showed slight activity. These results suggest that zPOMT2 itself has enzymatic activity, or zPOMT2 may form a complex with endogenous hPOMT1 resulting in low levels of enzymatic activity. Two heterologous protein combinations, zPOMT1 and hPOMT2 or zPOMT2 and hPOMT1, resulted in robust levels of enzymatic activity (Figure 5). This result suggests that a single mechanism of *O*-mannosylation is common to humans and zebrafish. On the other hand, cells co-transfected with *zPOMT1* and *hPOMT1* and cells co-transfected with *zPOMT2* and *hPOMT2* did not show any enzymatic activity, indicating clearly that POMT1 and POMT2 have different functional roles in POMT enzymatic activity. It is not clear why protein *O*-mannosyltransferase activity requires co-expression of POMT1 and POMT2 (Ichimiya et al. 2004; Manya et al. 2006; Manya et al. 2004); this study). One possibility is that POMT1 is a catalytic molecule and POMT2 is a regulatory molecule or vice versa. Another possibility is that assembly of POMT1 and POMT2 forms a catalytic domain. To further understand the mechanism of protein *O*-mannosylation, it is necessary to perform a structural study of a complex formed by POMT1 and POMT2.

Remarkably, overlapping expression patterns of *zPOMT1* and *zPOMT2* were observed by whole-mount in situ hybridization (Figure 3C). Such overlapping pattern suggests that the two proteins may collaborate functionally in vivo. This expression data are consistent with data suggesting that simultaneous expression of zPOMT1 and zPOMT2 is required for POMT enzymatic activity. Interestingly, similar co-expression of *POMTs* was observed in various tissues and during different developmental stages of embryogenesis in mouse and *Drosophila* (Ichimiya et al. 2004; Lyalin et al. 2006; Lommel et al. 2008). These results suggest that both protein *O*-mannosylation machinery and biological importance of protein *O*-mannosylation may have been conserved during metazoan evolution, although further analyses are necessary to understand the molecular mechanisms of protein *O*-mannosylation and its evolution.

The expression levels of the two *POMTs* genes differed at various developmental stages and in specific tissues of mouse, *Drosophila* and zebrafish. For example, while mouse *POMT2* was highly expressed in testis (Willer et al. 2002), *zPOMT1* and *zPOMT2* were highly expressed in ovary and testis (Figure 3B). Since *POMT1* knockout in mice results in embryonic lethality, protein *O*-mannosylation is necessary for normal development (Willer et al. 2004). In the case of *Drosophila POMTs*, the expression level of *dPOMT1* was higher than that of *dPOMT2* from 0 to 2 h in the embryo (Ichimiya et al. 2004), whereas the expression level of *zPOMT2* was higher than that of *zPOMT1* at from 0 to 6 hpf. It was assumed that both *zPOMT1* and *zPOMT2* mRNAs at these stages were derived

from maternal expression. Furthermore, the expression level of *zPOMT1* decreased from 0 to 6 hpf, whereas *zPOMT2* expression was high from 0 to 6 hpf (Figure 3A). These results suggest that the expression of *zPOMT1* and *zPOMT2* may be regulated differently.

In humans, defects of protein *O*-mannosylation lead to WWS (Manya et al. 2003; Akasaka-Manya et al. 2004). To understand the importance of protein *O*-mannosylation in zebrafish development, we carried out the knockdown analysis of antisense MOs against *zPOMT1* and *zPOMT2*. As a result, *zPOMT1* and *zPOMT2* morphant embryos showed curved tail, and some had edematous pericardium (Figure 4B). Since both *zPOMT1* and *zPOMT2* morphants showed these phenotypic aberrations, they could not swim straight or feed at all, and they eventually died. At 96 hpf, the phenotypes of *zPOMT2* morphant embryos showed a higher incidence of more severe phenotypes than the *zPOMT1* morphant embryos did (Table I), yet immunoreactivity of IIH6 in *zPOMT1* and *zPOMT2* morphants was similar (Figure 4C). We predicted that the phenotypes of zebrafish embryos injected with MOs against *zPOMT1* and *zPOMT2* would be the same or similar because the expression patterns of the two genes were similar before 24 hpf (Figure 3). Therefore, the difference of phenotypes observed between *zPOMT1* and *zPOMT2* morphants in early development of the zebrafish might be explained by the variance of knockdown efficiency or by another function of zPOMT2 in addition to enzymatic activity. It may be consistent with severe phenotypes observed in *zPOMT2* embryos that only *zPOMT2* morphant embryos showed aberrant pigmentation in eyes. Fukutin-deficient chimeric mice revealed abnormalities in eyes, indicating that corneal opacification with vascular infiltration and eye abnormality was quite remarkable according to their aberrant pigmentation (Takeda et al. 2003). Further studies are necessary to reveal the role of *O*-mannosylglycans in the pathogenesis of eye abnormalities.

Here, we demonstrated that zebrafish POMTs possess protein *O*-mannosyltransferase activity when co-expressed in HEK293T cells. This result suggested that the protein *O*-mannosylation machinery is conserved in mammals and zebrafish. Therefore, to elucidate whether the function and mechanism of protein *O*-mannosylation related to *POMTs* are evolutionarily conserved in the vertebrates, the zebrafish should be a useful model. It was also suggested that the zebrafish may be a useful model for understanding the functions of glycans in the whole body. In the knockdown analyses of *zPOMT1* and *zPOMT2* by MOs, no glycosylated α-DG was detected in 48 hpf embryos (Figure 4C). Therefore, it appears that the enzymatic activity was completely lost. Furthermore, zebrafish α-dystroglycanopathy models may be useful to search for chemicals that treat α-dystroglycanopathies; the simple addition of candidate molecules to water could be developed as assays for theraputic effectiveness.

Materials and methods

Zebrafish and embryos

Zebrafish adults were maintained at 28°C under light condition of 14 h light period and 10 h dark period. Embryos were collected from pair-wise mating of adults and kept in filter-sterilized fresh water at 28°C.

Cloning and sequencing of the full-length cDNAs

Total RNAs were purified from 24 and 48 hpf embryos by using QIAzol (Qiagen, Hilden, Germany), and cDNA fragments were generated by RT-PCR using oligo dT primer and Superscript II reverse transcriptase (Invitrogen Corp., Carlsbad, CA). Degenerated oligonucleotide primers were designed by mRNA sequence of zebrafish POMT1 (zPOMT1) (accession no. NM_001048067.2). zPOMT2 gene (accession no. AB281276) was cloned in a zebrafish embryonic cDNA library that was synthesized with a SMART cDNA Library Construction Kit (Clontech, Mountain View, CA). Both zPOMT1 and zPOMT2 genes were amplified with the forward primers, 5′-atgcagtgtgttaaactgcccgtcagtgt-3′ and 5′-atggatgtcagaccgaaggagaatttc-3′, and the reverse primers, 5′-ttagcgtttgcgtaagagaatatcccaactctc-3′ and 5′-ctaaaactcccaggattccatccacc-3′, respectively. The amplified cDNA fragments were cloned into pT7Blue vector (Novagen, Madison, WI), and the sequences were confirmed by CEQ™ 2000 DNA Analysis System (Beckman Coulter, Inc., Fullerton, CA) with a DTCS Quick Start kit (Beckman Coulter, Inc.). The nucleotide sequence was subjected to the basic local alignment with a BLAST search provided by the National Center for Biotechnology Information. The sequences were obtained from GenBank and aligned using CLUSTAL W (Thompson et al. 1994). A phylogenetic tree was generated using the neighbor-joining method. TREEVIEW software generated visual representations of clusters (Page 1996).

Quantitative PCR analyses

Total RNA was extracted from embryos at 0, 6, 12, 18, 24, 48, 72 and 96 hpf and the tissue samples (brain, heart, liver, kidney, spleen, intestine, muscle, testis and ovary) of either male or female adult zebrafish. One microgram of total RNA was used for cDNA synthesis. First-strand cDNA was synthesized as described in the section of *cDNA cloning and sequencing of zPOMT1 and zPOMT2*. Quantitative PCR was carried out with SYBR Green Realtime PCR Master Mix (TOYOBO Co. LTD., Osaka, Japan). Two microliters of cDNA (0.1 μg/μL) was used for a template. The primers used to detect the messages of *zPOMT1* and *zPOMT2* were 5′-tgttggctgtgctgtcttacc-3′ (forward) and 5′-catggctcaaggttcgatctc-3′ (reverse), 5′-cctcatgtatgttgggatgagac-3′ (forward) and 5′-gaaccaagagcagcacagaac-3′ (reverse), respectively. The primers for *zβ-actin2* and *zCox1*—5′-agttcagccatggatgatgaaa-3′ (forward) and 5′-accatgacaccctgatgtct-3′ (reverse), 5′-ttggccacccagaagtctac-3′ (forward) and 5′-gctcgggtgtctacatccat-3′ (reverse), respectively—were used as internal controls. Annealing temperatures were 63°C for *zPOMT1* and *zPOMT2*, 52°C for *zβ-actin2* and 54°C for *zCox1*. Melting curves were calibrated by LineGene (NIPPON Genetics Co. LTD., Tokyo, Japan).

Whole-mount in situ hybridization

Antisense probe synthesis was performed using a Digoxigenin (DIG) RNA Labeling Kit (Roche Diagnostics, Basel, Switzerland). Zebrafish embryos were collected after spawning and maintained at 28°C. Embryos at 0, 6, 12, 18, 24, 48, 72 and 96 hpf were fixed with 4% paraformaldehyde (PFA)-phosphate-buffered saline (PBS), dehydrated and kept in methanol

at −80°C. The embryos were rehydrated in PBS, and hybridization of a DIG-labeled RNA probe was carried out in a hybridization buffer containing 50% formamide, 25% 20×SSC, 1% Tween20, 9 mM citric acid and 1 mg/ml heparin at 65°C for 16 h. Embryos hybridized with a DIG-labeled RNA were incubated with anti-DIG antibody conjugated to alkaline phosphatase (Roche Diagnostics) (1:2000) at 4°C for 12 h, stained with BM purple (Roche Diagnostics) at room temperature for 2 h and fixed with 4% PFA-PBS. The embryos were observed using ECLIPSE E600 (Nikon Corp., Tokyo, Japan).

Localization of 3′UTRs in zPOMT1 and zPOMT2 genes

The *EGFP* gene was cloned into pSP72 vector (Promega, Madison, WI). The3′UTRs of *zPOMT1* and *zPOMT2* were fused separately downstream of *EGFP* gene. The 3′UTR of zebrafish *NUDT2* was used as a control. Capped mRNAs of *EGFP-zPOMTs-3′UTR* were synthesized using mMESSAGE mMACHINE High Yield Capped RNA Transcription Kit (SP6, Ambion Inc., Austin, TX). Capped mRNAs at a concentration of 0.05 μg/μL were injected into fertilized eggs from one to two cells. The embryos were observed until 24 hpf using ECLIPSE E600 and a mercury lamp (Nikon).

Knockdown analysis of zPOMT1 and zPOMT2

Antisense MOs targeted to interfere with *zPOMT1* and *zPOMT2* translation were purchased from Gene Tools LLC (Philomath, OR). The antisense sequences of *zPOMT1* and *zPOMT2* genes were designed using the 50 sequence around the putative start of translation of *zPOMT1* and *zPOMT2* mRNA (accession nos. AB281275 and AB281276). The morpholino sequences were *zPOMT1*-MO: 5′-gacgggcagtttaacacactgcatg-3′ and *zPOMT2*-MO: 5′-gtccattcttgaagatgaagaggac-3′. The sequence of control MO was 5′-gtacgtcacacaatttgacgggcag-3′. MOs at a concentration of 0.25, 0.5 or 1.0 mM were injected into embryos at the one- to two-cell stage.

Immunohistochemistry

For immunohistochemistry, embryos were fixed overnight in 4% paraformaldehyde solution, embedded in paraffin and sectioned at 10 μm and mounted on slides. Sections were left to dry for 2 h. After being dewaxed and rehydrated, some sections were stained with hematoxylin and eosin, while others were subjected to immunohistostaining as described in (Mulero et al. 2007). Anti-glycosylated α-DG IIH6 (Upstate, Millipore, Billerica, MA) was used at a dilution of 1:100 with PBS. Slides were washed 3× 10 min with PBS containing 0.1% Tween (PBSTw) and incubated with secondary antibody for 1 h. The secondary antibody used was Alexa Fluor 488 Goat Anti-Mouse IgM (Molecular Probes Invitrogen Life Technologoies Corp., Tokyo, Japan) at a dilution of 1:500 with PBS. Embryos were fixed in 4% PFA-PBS and transferred into 100% methanol. The embryos were rehydrated in PBS containing 0.1% Tween-20 (PBT) and incubated in PBT containing anti-glycosylated α-DG antibody (IIH6) overnight at 4°C followed by several washes with PBT and incubation with secondary antibody (goat anti-mouse IgM AlexaFluor-488,). The embryos were observed using ECLIPSE E600 and a mercury lamp (Nikon).

Assay for protein O-mannosyltransferase activity

Expression plasmids of zPOMT1 and zPOMT2 were constructed using pcDNA3.1 Hygro (+) vector (Life Technologoies Corp., Tokyo, Japan) and confirmed by the sequencing. The expression plasmids were transfected into HEK293T cells, and the cells were cultured for 3 days in complete medium, harvested, and homogenized. Protein *O*-mannosyltransferase activity was based on the amount of [^{3}H]-mannose transferred from [^{3}H]-mannosylphosphoryldolichol to a glutathione-S-transferase fusion α-DG (GST-α-DG) as described previously (Manya et al. 2004). Approximately 80 μg of microsomal membrane fractions were collected from HEK293T cells coexpressing combinations of *POMT1* and/or *POMT2* genes from either human or zebrafish, suspended in a 20-μL reaction buffer containing 10 μg of GST-α-DG. The reaction mixture was incubated at 22°C for 1 h, and GST-α-DG was purified using glutathione-Sepharose 4B beads (GE Healthcare Bio-Sciences Corp., Piscataway, NJ). The radioactivity adsorbed to the beads was measured by using liquid scintillation counter.

Acknowledgement

We would like to thank Dr. Roy H. Doi, Distinguished Professor Emeritus of Molecular Biology at the University of California, Davis, for his English corrections and discussion.

Funding

This work was supported by grants from the Wakayama Prefecture Collaboration of Regional Entities for the Advancement of Technological Excellence and SENTAN, Japan Science and the Technology Agency and the New Energy and Industrial Technology Development Organization (02A09003d), and Grant-in-Aid for Scientific Research (20370053) from the Japan Society for the Promotion of Science, a Research Grant for Nervous and Mental Disorders (20B-13) and Research on Psychiatric and Neurological Diseases and Mental Health from the Ministry of Health, Labor, and Welfare of Japan, and a grant from The Takeda Science Foundation.

The nucleotide sequences in this paper have been submitted to the Genbank/EMBL/DDBJ Nucleotide Sequence Database. The accession numbers AB281275 and AB281276 have been assigned to the cDNA sequences of zebrafish POMT1 and POMT2, respectively.

Abbreviations

α-DG, α-dystroglycan; DGC, dystrophin–glycoprotein complex; DIG, Digoxigenin; *EGFP, enhanced green fluorescent protein*; FKRP, fukutin-related protein; HEK293T cells, human embryonic kidney 293T cells; MO, morpholino oligonucleotide; ORF, open reading frame; PBS phosphate-buffered saline; PBT PBS containing 0.1% Tween-20; PFA paraformaldehyde; POMGnT1, protein *O*-mannose β1,2-*N*-acetylglucosaminyltransferase1; POMT, PMT, protein *O*-mannosyltransferase; RT-PCR, reverse transcriptase-polymease chain reaction; SD, standard deviation; WWS, Walker–Warburg syndrome.

References

Akasaka-Manya K, Manya H, Endo T. 2004. Mutations of the POMT1 gene found in patients with Walker–Warburg syndrome lead to a defect of protein *O*-mannosylation. *Biochem Biophys Res Commun.* 325:75–79.

Akasaka-Manya K, Manya H, Nakajima A, Kawakita M, Endo T. 2006. Physical and functional association of human protein *O*-mannosyltransferases 1 and 2. *J Biol Chem.* 281:19339–19345.

Bassett DI, Currie PD. 2003. The zebrafish as a model for muscular dystrophy and congenital myopathy. *Hum Mol Genet.* 12(Suppl.2): R265–R270.

Bassett DI, Bryson-Richardson RJ, Daggett DF, Gautier P, Keenan DG, Currie PD. 2003. Dystrophin is required for the formation of stable muscle attachments in the zebrafish embryo. *Development.* 130:5851–5860.

Beedle AM, Nienaber PM, Campbell KP. 2007. Fukutin-related protein associates with the sarcolemmal dystrophin–glycoprotein complex. *J Biol Chem.* 282:16713–16717.

Beltran-Valero de Bernabe D, Currier S, Steinbrecher A, Celli J, van Beusekom E, van der Zwaag B, Kayserili H, Merlini L, Chitayat D, Dobyns WB, et al. 2002. Mutations in the *O*-mannosyltransferase gene POMT1 give rise to the severe neuronal migration disorder Walker–Warburg syndrome. *Am J Hum Genet.* 71:1033–1043.

Burton EA, Davies KE. 2002. Muscular dystrophy—reason for optimism? *Cell.* 108:5–8.

Chiba A, Matsumura K, Yamada H, Inazu T, Shimizu T, Kusunoki S, Kanazawa I, Kobata A, Endo T. 1997. Structures of sialylated *O*-linked oligosaccharides of bovine peripheral nerve α-dystroglycan. The role of a novel *O*-mannosyl-type oligosaccharide in the binding of α-dystroglycan with laminin. *J Biol Chem.* 272:2156–2162.

Devoto SH, Melancon E, Eisen JS, Westerfield M. 1996. Identification of separate slow and fast muscle precursor cells in vivo, prior to somite formation. *Development.* 122:3371–3380.

Dolatshad NF, Brockington M, Torelli S, Skordis L, Wever U, Wells DJ, Muntoni F, Brown SC. 2005. Mutated fukutin-related protein (FKRP) localises as wild type in differentiated muscle cells. *Exp Cell Res.* 309:370–378.

Endo T. 1999. *O*-mannosyl glycans in mammals. *Biochim Biophys Acta.* 1473:237–246.

Endo T, Toda T. 2003. Glycosylation in congenital muscular dystrophies. *Biol Pharm Bull.* 26:1641–1647.

Esapa CT, Benson MA, Schröder JE, Martin-Rendon E, Brockington M, Brown SC, Muntoni F, Kröger S, Blake DJ. 2002. Functional requirements for fukutin-related protein in the Golgi apparatus. *Hum Mol Genet.* 11:3319–3331.

Esapa CT, McIlhinney RA, Blake DJ. 2005. Fukutin-related protein mutations that cause congenital muscular dystrophy result in ER-retention of the mutant protein in cultured cells. *Hum Mol Genet.* 14:295–305.

Guyon JR, Mosley AN, Zhou Y, O'Brien KF, Sheng X, Chiang K, Davidson AJ, Volinski JM, Zon LI, Kunkel LM. 2003. The dystrophin associated protein complex in zebrafish. *Hum Mol Genet.* 12:601–615.

Haltiwanger RS, Lowe JB. 2004. Role of glycosylation in development. *Annu Rev Biochem.* 73:491–537.

Hashimoto H, Kawaguchi S, Hara K, Nakamura K, Shimizu T, Tamaru Y, Sato M. 2009. Purification, crystallization and initial X-ray diffraction study of the zinc-finger domain of zebrafish Nanos. *Acta Crystallogr Sect F Struct Biol Cryst Commun.* 65:959–961.

Ichimiya T, Manya H, Ohmae Y, Yoshida H, Takahashi K, Ueda R, Endo T, Nishihara S. 2004. The twisted abdomen phenotype of *Drosophila* POMT1 and POMT2 mutants coincides with their heterophilic protein *O*-mannosyltransferase activity. *J Biol Chem.* 279:42638–42647.

Jurado LA, Coloma A, Cruces J. 1999. Identification of a human homolog of the *Drosophila* rotated abdomen gene (POMT1) encoding a putative protein *O*-mannosyltransferase, and assignment to human chromosome 9q34.1. *Genomics.* 58:171–180.

Krusius T, Finne J, Margolis RK, Margolis RU. 1986. Identification of an *O*-glycosidic mannose-linked sialylated tetrasaccharide and keratan sulfate oligosaccharides in the chondroitin sulfate proteoglycan of brain. *J Biol Chem.* 261:8237–8242.

Liu J, Ball SL, Yang Y, Mei P, Zhang L, Shi H, Kaminski HJ, Lemmon VP, Hu H. 2006. A genetic model for muscle–eye–brain disease in mice lacking protein O-mannose 1, 2-N-acetylglucosaminyltransferase (POMGnT1). *Mech Dev.* 123:228–240.

Lommel M, Willer T, Strahl S. 2008. POMT2, a key enzyme in Walker-Warburg syndrome: somatic *sPOMT2*, but not testis-specific *tPOMT2*, is crucial for mannosyltransferase activity in vivo. *Glycobiology.* 18:615–625.

Lyalin D, Koles K, Roosendaal SD, Repnikova E, Van Wechel L, Panin VM. 2006. The *twisted* gene encodes *Drosophila* protein *O*-mannosyltransferase 2 and genetically interacts with the *rotated abdomen* gene encoding *Drosophila* protein *O*-mannosyltransferase 1. *Genetics.* 172:343–353.

Manya H, Chiba A, Margolis RU, Endo T. 2006. Molecular cloning and characterization of rat Pomt1 and Pomt2. *Glycobiology.* 16:863–873.

Manya H, Chiba A, Yoshida A, Wang X, Chiba Y, Jigami Y, Margolis RU, Endo T. 2004. Demonstration of mammalian protein *O*-mannosyltransferase activity: coexpression of POMT1 and POMT2 required for enzymatic activity. *Proc Natl Acad Sci USA.* 101:500–505.

Manya H, Sakai K, Kobayashi K, Taniguchi K, Kawakita M, Toda T, Endo T. 2003. Loss-of-function of an *N*-acetylglucosaminyltransferase, POMGnT1, in muscle-eye- brain disease. *Biochem Biophys Res Commun.* 306:93–97.

Martín-Blanco E, García-Bellido A. 1996. Mutations in the rotated abdomen locus affect muscle development and reveal an intrinsic asymmetry in *Drosophila*. *Proc Natl Acad Sci USA.* 93:6048–6052.

Matsumoto H, Noguchi S, Sugie K, Ogawa M, Murayama K, Hayashi YK, Nishino I. 2004. Subcellular localization of fukutin and fukutin-related protein in muscle cells. *J Biochem (Tokyo).* 135:709–712.

Michele DE, Campbell KP. 2003. Dystrophin-glycoprotein complex: post-translational processing and dystroglycan function. *J Biol Chem.* 278: 15457–15460.

Miyagoe-Suzuki Y, Masubuchi N, Miyamoto K, Wada M, Yuasa S, Saito F, Matsumura K, Kanesaki H, Kudo A, Manya H, et al. 2009. Reduced proliferative activity of primary POMGnT1-null myoblasts *in vitro*. *Mech Dev.* 126:107–116.

Montanaro F, Carbonetto S. 2003. Targeting dystroglycan in the brain. *Neuron.* 37:193–196.

Moore CJ, Goh HT, Hewitt J. 2008. Genes required for functional glycosylation of dystroglycan are conserved in zebrafish. *Genomics.* 92:159–167.

Mulero I, Sepulcre MP, Meseguer J, García-Ayala A, Mulero V. 2007. Histamine is stored in mast cells of most evolutionarily advanced fish and regulates the fish inflammatory response. *Proc Natl Acad Sci USA.* 104:19434–19439.

Ohtsubo K, Marth JD. 2006. Glycosylation in cellular mechanisms of health and disease. *Cell.* 126:855–867.

Page RD. 1996. TreeView: an application to display phylogenetic trees on personal computers. *Comput Appl Biosci.* 12:357–358.

Parsons MJ, Campos I, Hirst EM, Stemple DL. 2002. Removal of dystroglycan causes severe muscular dystrophy in zebrafish embryos. *Development.* 129:3505–3512.

Sasaki T, Yamada H, Matsumura K, Shimizu T, Kobata A, Endo T. 1998. Detection of *O*-mannosyl glycans in rabbit skeletal muscle α-dystroglycan. *Biochim Biophys Acta.* 1425:599–606.

Steffen LS, Guyon JR, Vogel ED, Beltre R, Pusack TJ, Zhou Y, Zon LI, Kunkel LM. 2007. Zebrafish orthologs of human muscular dystrophy genes. *BMC Genomics.* 8:79.

Strahl-Bolsinger S, Tanner W. 1991. Protein *O*-glycosylation in *Saccharomyces cerevisiae*. Purification and characterization of the dolichylphosphate-D-mannose- protein *O*-D-mannosyltransferase. *Eur J Biochem.* 196:185–190.

Takeda S, Kondo M, Sasaki J, Kurahashi H, Kano H, Arai K, Misaki K, Fukui T, Kobayashi K, Tachikawa M, et al. 2003. Fukutin is required for maintenance of muscle integrity, cortical histiogenesis and normal eye development. *Hum Mol Genet.* 12:1449–1459.

Thompson JD, Higgins DG, Gibson TJ. 1994. CLUSTAL W: improving the sensitivity of progressive multiple sequence alignment through sequence weighting, position-specific gap penalties and weight matrix choice. *Nucleic Acids Res.* 22:4673–4680.

Thornhill P, Bassett D, Lochmüller H, Bushby K, Straub V. 2008. Developmental defects in a zebrafish model for muscular dystorophies associated with the loss of fukutin-related protein (FKRP). *Brain.* 131:1551–1561.

Torelli S, Brown SC, Brockington M, Dolatshad NF, Jimenez C, Skordis L, Feng LH, Merlini L, Jones DH, Romero N, et al. 2005. Sub-cellular localization of fukutin related protein in different cell lines and in the muscle of patients with MDC1C and LGMD2I. *Neuromuscul Disord.* 15:836–843.

van Reeuwijk J, Janssen M, van den Elzen C, Beltran-Valero de Bernabe D, Sabatelli P, Merlini L, Boon M, Scheffer H, Brockington M, Muntoni F, et al. 2005. POMT2 mutations cause α-dystroglycan hypoglycosylation and Walker–Warburg syndrome. *J Med Genet.* 42:907–912.

Willer T, Amselgruber W, Deutzmann R, Strahl S. 2002. Characterization of POMT2, a novel member of the PMT protein *O*-mannosyltransferase family specifically localized to the acrosome of mammalian spermatids. *Glycobiology.* 12:771–783.

Willer T, Prados B, Falcon-Peres JM, Renner-Muller I, Przemech GK, Lommel M, Coloma A, Valero MC, de Angelis MH, Tanner W, et al. 2004. Targeted disruption of the Walker–Warburg syndrome gene Pomt1 in mouse result in embryonic lethality. *Proc Natl Acad Sci USA*. 101:14126–14131.

Yoshida A, Kobayashi K, Manya H, Taniguchi K, Kano H, Mizuno M, Inazu T, Mitsuhashi H, Takahashi S, Takeuchi M, et al. 2001. Muscular dystrophy and neuronal migration disorder caused by mutations in a glycosyltransferase, POMGnT1. *Dev Cell*. 1:717–724.

Biochemical and Biophysical Research Communications 410 (2011) 632–636

Contents lists available at ScienceDirect

Biochemical and Biophysical Research Communications

journal homepage: www.elsevier.com/locate/ybbrc

Effects of length and amino acid sequence of *O*-mannosyl peptides on substrate specificity of protein *O*-linked mannose β1,2-*N*-acetylglucosaminyltransferase 1 (POMGnT1)

Keiko Akasaka-Manya [a], Hiroshi Manya [a], Mamoru Mizuno [b], Toshiyuki Inazu [c], Tamao Endo [a,*]

[a] *Molecular Glycobiology, Research Team for Mechanism of Aging, Tokyo Metropolitan Institute of Gerontology, Tokyo Metropolitan Geriatric Hospital and Institute of Gerontology, 35-2 Sakaecho, Itabashi-ku, Tokyo 173-0015, Japan*
[b] *Laboratory of Glyco-organic Chemistry, The Noguchi Institute, Itabashi-ku, Tokyo 173-0003, Japan*
[c] *Department of Applied Chemistry, School of Engineering and Institute of Glycotechnology, Tokai University, Hiratsuka-shi, Kanagawa 259-1292, Japan*

ARTICLE INFO

Article history:
Received 20 May 2011
Available online 13 June 2011

Keywords:
POMGnT1
Substrate specificity
Glycosyltransferase
Kinetic analysis
Baculovirus/insect cell expression system

ABSTRACT

Protein *O*-linked mannose β1,2-*N*-acetylglucosaminyltransferase 1 (POMGnT1) catalyzes the transfer of GlcNAc to *O*-mannose of glycoproteins. Mutations in the *POMGnT1* gene cause muscle–eye–brain disease (MEB). POMGnT1 is a typical type II membrane protein, which is localized in the Golgi apparatus. However, details of the catalytic and reaction mechanism of POMGnT1 are not understood. To develop a better understanding of POMGnT1, we examined the substrate specificity of POMGnT1 using a series of synthetic *O*-mannosyl peptides based on the human α-dystroglycan (α-DG) sequence as substrates. *O*-Mannosyl peptides consisting of three to 20 amino acids are recognized as substrates. Enzyme kinetics improved with increasing peptide length up to a length of 8 amino acids but the kinetics of peptides longer than 8 amino acids were similar to those of octapeptides. Our results also show that the amino acid sequence affects POMGnT1 activity. These data suggest that both length and amino acid sequence of mannosyl peptides are determinants of POMGnT1 substrate specificity.

1. Introduction

Protein *O*-linked mannose β1,2-*N*-acetylglucosaminyltransferase 1 (POMGnT1) catalyzes the transfer of GlcNAc to *O*-mannose of glycoproteins. POMGnT1 is responsible for muscle–eye–brain disease (MEB), which is an autosomal recessive disorder characterized by congenital muscular dystrophy, ocular abnormality, and brain malformation. The human *POMGnT1* gene was cloned from a cDNA sequence homologous to human *GnT-I* (UDP-GlcNAc: α-3-D-mannoside β1,2-*N*-acetylglucosaminyltransferase I). Although the overall amino acid sequence identity of POMGnT1 and GnT-I was only 23.2%, the predicted catalytic domains of both are highly homologous [1]. Such high conservation of the catalytic domain suggests that the reaction mechanism of POMGnT1 is partly similar to that of GnT-I. POMGnT1 and GnT-I are typical type II membrane proteins that are localized in the Golgi apparatus, and both enzymes form GlcNAcβ1–2Man linkages. A difference is that POMGnT1 catalyzes the GlcNAcβ1–2Man linkage in *O*-mannosyl glycans but not in *N*-glycans, while GnT-I catalyzes the same linkage in *N*-glycans but not in *O*-mannosyl glycans. The reason for these specificities is unclear.

Mammalian POMGnT1 is known to recognize synthetic mannosyl-peptide and benzyl-α-D-mannose as an acceptor [1,2], but not free mannose or *p*-nitrophenyl-α-mannose [1]. Thus, in order for POMGnT1 to recognize mannose, the mannose must be linked to certain other moieties.

It is known that two distinct *O*-fucosyl glycan-processing pathways exist: one is specific for epidermal growth factor-like (EGF) repeats and the other is specific for thrombospondin type 1 repeats (TSRs) [3,4]. *O*-Fucose-specific β1,3-*N*-acetylglucosaminyltransferase is able to modify *O*-fucose on an EGF repeat but not on a TSR, while *O*-fucose-specific β1,3-glucosyltransferase is able to modify *O*-fucose on a TSR but not on an EGF repeat. These results suggest that enzymes responsible for elongation of glycan following *O*-fucose are different and that each elongation enzyme strictly recognizes a particular amino acid sequences or conformation. These unique specificities of the two elongation enzymes prompted us to examine whether adding GlcNAc to *O*-mannose by POMGnT1 depends on the amino acid sequence near the *O*-mannosylated site. To answer this question, we analyzed the substrate specificity of POMGnT1 using a series of synthetic *O*-mannosyl peptides.

2. Materials and methods

2.1. Materials

O-Mannosyl peptides were synthesized in a solid-phase manner using 9-fluorenylmethyloxycarbonyl (Fmoc) chemistry [5]. The

* Corresponding author. Fax: +81 3 3579 4776.
E-mail address: endo@tmig.or.jp (T. Endo).

0006-291X/$ - see front matter © 2011 Elsevier Inc. All rights reserved.
doi:10.1016/j.bbrc.2011.06.042

structures of each mannosyl peptide were identified by ^{1}H NMR, amino acid analysis (6 M HCl, 110 °C, 24 h) and matrix-assisted laser desorption ionization time-of-flight mass spectrometry (MALDI-TOF MS).

2.2. Preparation of recombinant baculovirus and expression of soluble His-POMGnT1

The soluble form of human POMGnT1 used as an enzyme source was prepared using the baculovirus (*Autographa californica nucleopolyhedro virus*) expression vector system (Nosan Corporation, Kanagawa, Japan; Protein Sciences Corporation, Meridien, CT). The soluble POMGnT1 (Ser66-Thr660) fused His-tag and PreScission protease cleavage site (Leu-Glu-Val-Leu-Phe-Gln-Gly-Pro) was secreted from *expres*SF+ Insect cells (Protein Sciences Corp.) by using the Ig kappa chain secretion signal (Fig. 1A). The transfer vector for generating recombinant baculovirus was constructed by ligating two PCR products. The primer pairs and template plasmid DNAs were: fragment 1 encoding the secretion signal, His-tag epitope and protease cleavage site, 5′-GATCTAGAATGGAGACAGACACAC-3′, 5′-CTGGTACCGGGCCCCTGGAACAGAACTTCCAGATGATGATGATGA TGATGAG-3′ and *HX-sPOMGnT1/pcDNA3.1 Zeo*(+) [1]; fragment 2 encoding Ser66-Thr660 of POMGnT1, 5′-CCCGGTACCAGTGAAGCC AATGAAGACCC-3′, 5′-TAAGATCTTCATGTCTGTTCTGGGGCTCC-3′ and the *POMGnT1/pcDNA3.1 Zeo*(+) [1]. The *pcDNA3.1 Zeo*(+) was purchased from Invitrogen (Carlsbad, CA). Two fragments were ligated at an *Acc65* I site and introduced into the *Xba* I site and *Bgl* II sites of *pPSC8* (Protein Sciences Corp.). The recombinant baculovirus was produced by baculovirus expression vector system using transfer vector and *expres*SF+ cells according to the manufacturer's instructions (Protein Sciences Corp.). The single clones of the recombinant baculovirus were isolated and expanded, and the high titer (>10^8 pfu/ml) virus stock was prepared. Isolation of clones and determination of virus titers were performed by plaque assay. The *expres*SF+ cells were maintained in Sf900-II medium (Invitrogen) supplemented with 50 μg/ml Kanamycin at 27 °C. A 10-l culture of *expres*SF+ cells was infected with 10 ml of virus stock and incubated for 72 h to express soluble His-POMGnT1 protein.

2.3. Purification of recombinant human POMGnT1

The recovered 10-l culture medium was concentrated 100-fold by 50 kDa cut-off VIVAFLOW, ultrafiltration membrane (Sartorius AG, Goettingen, Germany). The collected medium (approximately 100 ml) was first subjected to Ni^{2+}-chelating Sepharose (HisTrap HP 5 ml, GE Healthcare UK Ltd., Buckinghamshire, England). After washing with 100 ml of 20 mM sodium phosphate buffer (pH 7.0) containing 300 mM NaCl and 20 mM imidazole, recombinant His-POMGnT1 was eluted from the column with 25 ml of 20 mM sodium phosphate buffer (pH 7.0) containing 300 mM NaCl and 500 mM imidazole. After dialysis against 20 mM sodium phosphate buffer (pH 7.0) containing 300 mM NaCl, the eluted enzyme was incubated with 250 μl of PreScission protease (GE Healthcare) and 250 μl of 100 mM dithiothreitol at 4 °C for 4 h to eliminate His-tag from His-POMGnT1. After PreScission protease digestion, recombinant POMGnT1 was subjected to the tandem columns combination of HisTrap column and Glutathione Sepharose column (GSTrap HP, GE Healthcare). The recombinant POMGnT1 was recovered in unbound fraction from the tandem columns by using 20 mM sodium phosphate (pH 7.0) containing 300 mM NaCl for washing buffer. The purity of recombinant POMGnT1 of each step was confirmed by SDS–PAGE.

2.4. Assay for POMGnT1 activity

POMGnT1 activity was obtained from the amount of [^{3}H] GlcNAc transferred to a substrate [1]. The reaction buffer containing 140 mM MES buffer (pH 7.0), 2 mM UDP-[^{3}H] GlcNAc

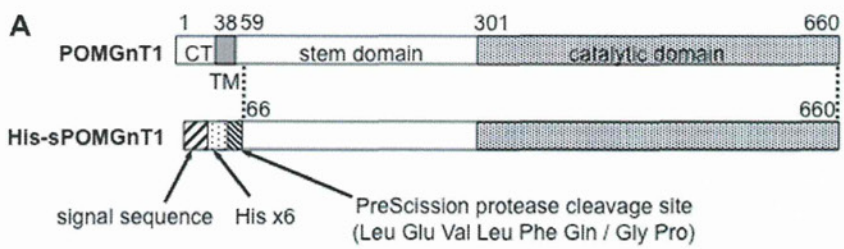

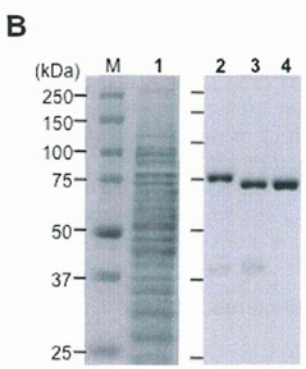

C

Purification of recombinant human POMGnT1

step	Specific activity (nmol/h/μg)
1. Culture medium	0.01
2. Ni^{2+}-affinity column	2.5
3. PreScission protease digested	2.6
4. Purified after the tandem columns	3.0

Fig. 1. (A) Schematic representation of human POMGnT1 and recombinant soluble POMGnT1 used in this study. POMGnT1 is a typical type II membrane protein, which is composed of, in order from the N-terminus, a cytoplasmic tail (CT), transmembrane domain (TM), stem domain, and catalytic domain. To prepare soluble enzyme, amino acid residues 1–65 were replaced by the sequence of the signal sequence, His tag, and PreScission protease cleavage site. The numbers above the boxes indicate the amino acid residue numbers of human POMGnT1. (B), (C) Electrophoretic patterns and POMGnT1 activity of recombinant human POMGnT1 at each purification step. Specific activity was determined using mannosyl nonapeptide. Lane 1, culture medium; lane 2, Ni^{2+}-affinity column absorbed protein; lane 3, PreScission protease-digested protein; lane 4, recombinant human POMGnT1 purified by tandem HisTrap and Glutathione Sepharose columns.

(50,000 dpm/nmol), 0.25–8 mM substrate, 10 mM $MnCl_2$, 2% Triton X-100, 5 mM AMP, 200 mM GlcNAc, 10% glycerol and enzyme solution was incubated at 37 °C for 1 h. After boiling for 3 min, the mixture was analyzed by reversed phase HPLC with a Wakopak 5C18–200 column (4.6 × 250 mm). Solvent A was 0.1% trifluoroacetic acid in distilled water and solvent B was 0.1% trifluoroacetic acid in acetonitrile. The peptide was eluted at a flow rate of 1 ml/min using a linear gradient of 1–25% solvent B. The peptide separation was monitored continuously at 214 nm, and the radioactivity of each fraction was measured using a liquid scintillation counter. *Km* and *Vmax* values were calculated on the basis of Hanes–Woolf plot.

3. Results and discussion

To produce recombinant human POMGnT1 on a large scale, we expressed a soluble form of the enzyme using a baculovirus/insect cell expression system. The recombinant human POMGnT1 used in the study lacked the cytoplasmic tail and transmembrane domain and included an *Ig* kappa chain secretion signal and His-tag at N-terminus (Fig. 1A). In order to remove the His-tag after Ni^{2+}-affinity chromatography, a protease digestion sequence (PreScission protease cleavage site) was inserted behind the His-tag region. Recombinant soluble POMGnT1 was produced in insect *expres*SF+ cells (Fig. 1B, lane 1) and purified from the culture medium by Ni^{2+}-affinity chromatography (lane 2). After cleavage of the His-tag, the protein migrated as a 70 kDa protein (lane 3). The protein was then cleaned up with tandem HisTrap and Glutathione Sepharose columns (lane 4). Ni^{2+}-affinity chromatography was very effective, increasing the specific activity of POMGnT1 by about three orders of magnitude (Fig. 1C). The final activity was high (3.0 nmol/h/μg) despite the removal of amino acid residues 1–65 from human POMGnT1 (Fig. 1A). This was expected because the minimal catalytic domain of POMGnT1 is located between positions 299 and 651 [6].

To examine the effect of peptide length on substrate specificity, we synthesized a series of mannosyl peptides consisting of a single mannosylated threonine residue and three to 20 amino acids (Fig. 2). The tri-, tetra-, hexa-, hepta-, octa- and deca-peptides were derived from mannosyl nonapeptide. The latter was based on amino acid residues 316–324 of α-DG in which most of threonine residues were substituted with alanine. Acetyl and amino groups were added to the termini of some mannosyl peptides to prevent their degradation during incubation. Mannosyl icosapeptide is based on amino acid residues 401–420 of α-DG which was found to act as a good substrate for protein *O*-mannosyl transferase [7]. The alanine-substituted mannosyl nonapeptide was designed to examine the effect of amino acid sequence on the enzymatic activity. We also examined benzyl-α-D-mannose as a substrate [2].

POMGnT1 activities with the different substrates were determined in Hanes-Woolf plots (Fig. 3) to obtain *Km* and *Vmax* values. *Vmax* and the catalytic constant *Kcat* were found to increase and *Km* was found to decrease with increasing peptide lengths for lengths up to 8 amino acids, although the hexapeptide was an exception (Table 1). For peptides longer than 8 amino acids, however, the kinetics were similar to those of octapeptides. Adding an alanine residue to the C-terminus of the hexapeptide (to form heptapeptide-I) decreased *Km* and *Vmax*, while adding an alanine to the N-terminus of the hexapeptide (to form heptapeptide-II) decreased *Km* even more and changed *Vmax* only slightly. These results suggest that four amino acids at the N-terminus make a better acceptor than three amino acids at the N-terminus. The finding that *Km* of alanine-substituted mannosyl nonapeptide is almost twice that of the original mannosyl nonapeptide (Table 1) shows that the amino acid sequence is also important.

Benzyl-α-D-mannose has a smaller *Km* than mannosyl heptapeptides, although its *Vmax* and *Kcat* values were similar to those of mannosyl tripeptide (Table 1). Benzyl-α-D-mannose's small *Km* may be due to its smaller molecular size, which could make it more difficult to release the product, benzyl-α-D-mannose-GlcNAc, from the catalytic pocket of the enzyme. POMGnT1 transferred GlcNAc to benzyl-α-D-mannose [2] but, as we found previously, not to either mannose or *p*-nitrophenyl-α-mannose [1], which suggests that the hydrophobicity of the benzyl group helps it to be recognized by the catalytic pocket of the enzyme.

X-ray crystal structure studies of POMGnT1 are needed to better understand the catalytic domain of the enzyme. Such studies have been used to determine the structures of many glycosyltransferases including GnT-I [8]. To crystallize the enzyme, a large amount of pure recombinant protein is needed. The expression system

Fig. 2. POMGnT1 substrates used in this study. Ac and NH_2 indicate acetyl and amino groups of the N- and C-termini, respectively. H and OH indicate that the peptides are not blocked.

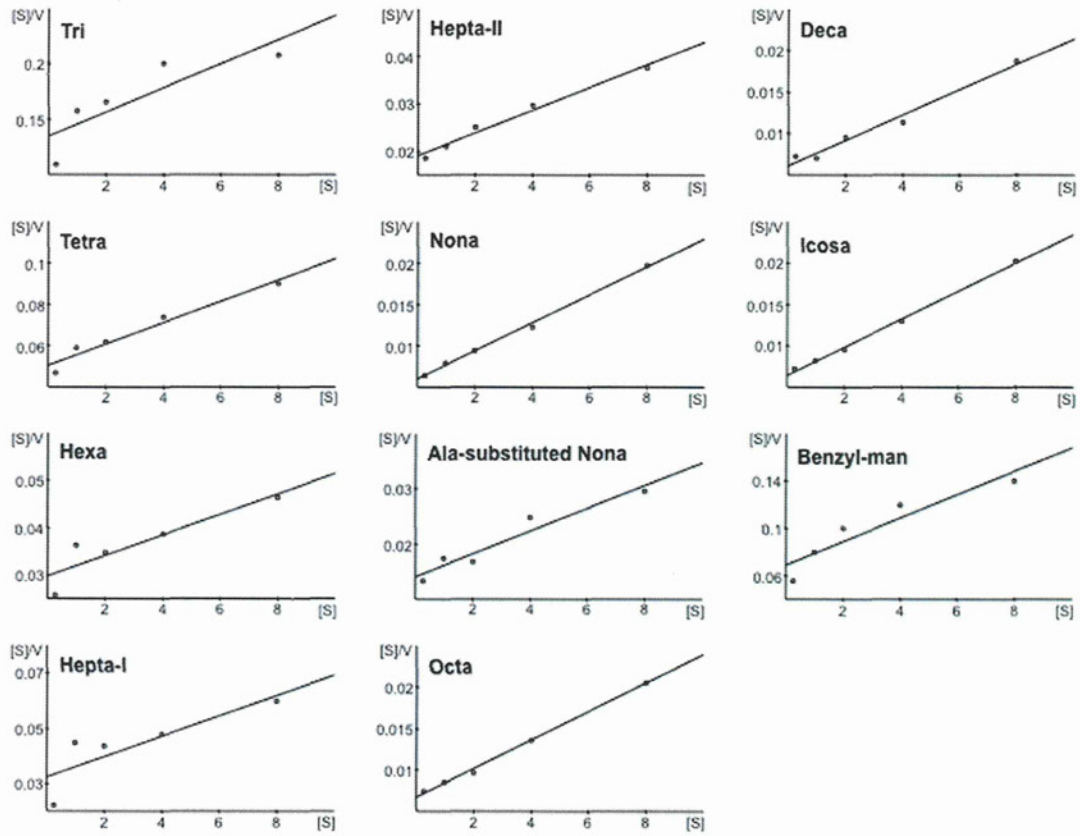

Fig. 3. Kinetic analysis of the purified recombinant POMGnT1 by Hanes-Woolf plot. The enzyme assay for POMGnT1 reaction is described in the Materials and methods. The kinetic parameters of POMGnT1 are summarized in Table 1. S, concentration of acceptor peptide (mM); V, specific activity (pmol/h/mg total protein).

Table 1
Kinetic parameters of POMGnT1 for various substrates.

Substrate	Sequence	MW	*Km* (mM)	*Vmax* (nmol/min/mg)	*Kcat* (1/s)
Tri	PT(Man)P	516	12.4	92	0.12
Tetra	PT(Man)PV	616	9.8	194	0.24
Hexa	TPT(Man)PVT	777	13.7	463	0.58
Hepta-I	TPT(Man)PVTA	848	8.8	271	0.34
Hepta-II	ATPT(Man)PVT	848	7.9	417	0.52
Ala-substituted Nona	AAAT(Man)AAAAP	917	6.8	483	0.60
Octa	ATPT(Man)PVTA	919	3.9	582	0.73
Nona	AAPT(Man)PVAAP	997	3.6	594	0.74
Deca	ATPT(Man)PVTAIG	1089	4.0	657	0.82
Icosa	IRPTMTIPGYVEPT(Man)AVATPP	2273	3.8	590	0.74
Benzyl-man		270	6.9	101	0.13

reported here, which can produce approximately 20 mg protein from 10 l of culture medium, is well suited for this task.

The regulatory mechanism of glycan processing is complicated and poorly understood. Some glycosyltransferases are known to modify specific regions of proteins. For example, two distinct *O*-fucosylation pathways exist [3,4]. EGF repeats in proteins are *O*-fucosylated by protein *O*-fucosyltransferase1 (Pofut1), and elongated by Fringe, a β1,3-*N*-acetylglucosaminyltransferase, while TSR repeats are *O*-fucosylated by a different *O*-fucosyltransferase, Pofut2, and then elongated by β1,3-glucosyltransferase [4,9]. These results indicate that these elongation enzymes recognize particular amino acid sequences or conformations. Our results (Table 1) also indicate that elongation of *O*-mannosyl glycans depends on the amino acid sequence. Recent studies have determined some of the *O*-mannosyl glycan structures and *O*-mannosylation sites on α-DG [10,11] but do not exclude the possibility that some *O*-mannose residues are not elongated. Further studies on all of the *O*-mannosyl glycan structures and *O*-mannosylation sites on α-DG will help to elucidate POMGnT1 substrate specificity.

Acknowledgments

This study was supported by a Grant-in-Aid for Scientific Research (20370053) from the Japan Society for the Promotion of Science, a Research Grant (20B-13) for Nervous and Mental Disorders, a Comprehensive Research on Disability Health and Welfare from the Ministry of Health (H22-021, H20-016), a Grant from The Naito Foundation, and a Grant from The Research Foundation for Pharmaceutical Sciences.

References

[1] A. Yoshida, K. Kobayashi, H. Manya, K. Taniguchi, H. Kano, M. Mizuno, T. Inazu, H. Mitsuhashi, S. Takahashi, M. Takeuchi, R. Herrmann, V. Straub, B. Talim, T. Voit, H. Topaloglu, T. Toda, T. Endo, Muscular dystrophy and neuronal migration disorder caused by mutations in a glycosyltransferase, POMGnT1, Dev. Cell 1 (2001) 717–724.

[2] W. Zhang, J. Vajsar, P. Cao, G. Breningstall, C. Diesen, W. Dobyns, R. Herrmann, A.E. Lehesjoki, A. Steinbrecher, B. Talim, T. Toda, H. Topaloglu, T. Voit, H. Schachter, Enzymatic diagnostic test for Muscle-Eye-Brain type congenital muscular dystrophy using commercially available reagents, Clin. Biochem. 36 (2003) 339–344.

[3] Y. Luo, K. Koles, W. Vorndam, R.S. Haltiwanger, V.M. Panin, Protein *O*-fucosyltransferase 2 adds *O*-fucose to thrombospondin type 1 repeats, J. Biol. Chem. 281 (2006) 9393–9399.

[4] Y. Luo, A. Nita-Lazar, R.S. Haltiwanger, Two distinct pathways for *O*-fucosylation of epidermal growth factor-like or thrombospondin type 1 repeats, J. Biol. Chem. 281 (2006) 9385–9392.

[5] S. Takahashi, T. Sasaki, H. Manya, Y. Chiba, A. Yoshida, M. Mizuno, H. Ishida, F. Ito, T. Inazu, N. Kotani, S. Takasaki, M. Takeuchi, T. Endo, A new beta-1,2-*N*-acetylglucosaminyltransferase that may play a role in the biosynthesis of mammalian *O*-mannosyl glycans, Glycobiology 11 (2001) 37–45.

[6] K. Akasaka-Manya, H. Manya, K. Kobayashi, T. Toda, T. Endo, Structure-function analysis of human protein *O*-linked mannose beta1, 2-*N*-acetylglucosaminyltransferase 1, POMGnT1, Biochem. Biophys. Res. Commun. 320 (2004) 39–44.

[7] H. Manya, T. Suzuki, K. Akasaka-Manya, H.K. Ishida, M. Mizuno, Y. Suzuki, T. Inazu, N. Dohmae, T. Endo, Regulation of mammalian protein *O*-mannosylation: preferential amino acid sequence for *O*-mannose modification, J. Biol. Chem. 282 (2007) 20200–20206.

[8] U.M. Unligil, S. Zhou, S. Yuwaraj, M. Sarkar, H. Schachter, J.M. Rini, X-ray crystal structure of rabbit *N*-acetylglucosaminyltransferase I: catalytic mechanism and a new protein superfamily, EMBO J. 19 (2000) 5269–5280.

[9] K. Kozma, J.J. Keusch, B. Hegemann, K.B. Luther, D. Klein, D. Hess, R.S. Haltiwanger, J. Hofsteenge, Identification and characterization of a beta1, 3-glucosyltransferase that synthesizes the Glc-beta1,3-Fuc disaccharide on thrombospondin type 1 repeats, J. Biol. Chem. 281 (2006) 36742–36751.

[10] J. Nilsson, G. Larson, A. Grahn, Characterization of site-specific *O*-glycan structures within the mucin-like domain of alpha-dystroglycan from human skeletal muscle, Glycobiology 20 (2010) 1160–1169.

[11] S.H. Stalnaker, S. Hashmi, J.M. Lim, K. Aoki, M. Porterfield, G. Gutierrez-Sanchez, J. Wheeler, J.M. Ervasti, C. Bergmann, M. Tiemeyer, L. Wells, Site mapping and characterization of *O*-glycan structures on alpha-dystroglycan isolated from rabbit skeletal muscle, J. Biol. Chem. 285 (2010) 24882–24891.

Biochemical and Biophysical Research Communications 411 (2011) 721–725

Contents lists available at ScienceDirect

Biochemical and Biophysical Research Communications

journal homepage: www.elsevier.com/locate/ybbrc

Different roles of the two components of human protein *O*-mannosyltransferase, POMT1 and POMT2

Keiko Akasaka-Manya, Hiroshi Manya, Masami Hayashi, Tamao Endo *

Molecular Glycobiology, Research Team for Mechanism of Aging, Tokyo Metropolitan Institute of Gerontology, Foundation for Research on Aging and Promotion of Human Welfare, 35-2 Sakaecho, Itabashi-ku, Tokyo 173-0015, Japan

ARTICLE INFO

Article history:
Received 24 June 2011
Available online 18 July 2011

Keywords:
Walker-Warburg syndrome
Muscular dystrophy
Glycosyltransferase
Protein O-mannosyltransferase

ABSTRACT

Protein *O*-mannosyltransferase 1 (POMT1) and its homolog, POMT2, are responsible for the catalysis of the first step in O-mannosyl glycan synthesis. Mutations in their genes are associated with a type of congenital muscular dystrophy called Walker-Warburg syndrome. Arg^{64}, Glu^{78} and Arg^{138} in the N-terminus region of ScPmt1p, a POMT homolog in *Saccharomyces cerevisiae*, are important for transferase activity. Arg^{138} is also essential for complex formation with ScPmt2p. Here we examined the effects of replacing the corresponding residues in human POMT1 and POMT2 with Ala on complex formation and enzymatic activity. The human POMT1 mutants lost almost all transferase activity while the POMT2 mutants retained enzymatic activity. Neither mutant lost its ability to form complexes with the native counter component. These results indicate that ScPmtps and human POMTs have different mechanisms of complex formation. They also suggest that human POMT1 and POMT2 have discrete functions since the effect of amino acid substitutions on enzymatic activity are different.

1. Introduction

Protein *O*-mannosyltransferase 1 (POMT1) and POMT2 (POMT, EC 2.4.1.109) catalyze the initial step of the biosynthesis of *O*-mannosyl glycans, in which a mannosyl residue is transferred from dolichyl phosphate mannose (Dol-P-Man) to Ser/Thr residues of certain proteins [1]. Complex formation of POMT1 and POMT2 is indispensable for POMT activity [1,2]. α-Dystroglycan (α-DG) is predominantly glycosylated by *O*-mannosyl glycan Siaα2-3Galβ1-4GlcNAcβ1-2Man [3]. α-DG consists of a dystrophin–glycoprotein complex that acts as a transmembrane linker between the extracellular matrix and intracellular cytoskeleton [4]. Defects in *O*-mannosyl glycans on α-DG are reported to cause several α-dystroglycanopathies, which are a group of congenital muscular dystrophies that include Walker-Warburg syndrome (WWS: OMIM 236670) [5,6]. Mutations in the *POMT1* and *POMT2* genes were identified in patients with WWS [7–10], an autosomal recessive developmental disorder associated with congenital muscular dystrophy, neuronal migration defects and ocular abnormalities. We previously demonstrated that these mutations almost abolished POMT activity and α-DG glycosylation [2,9]. However, how mutations cause a loss of POMT activity remains unclear.

O-Mannosylation is an essential protein modification that is evolutionarily conserved from eukaryotes to mycobacteria [11,12]. *O*-Mannosylation is essential for maintaining cell shape and cell integrity [13] and contributes to quality control of proteins in the ER in yeast [14,15]. Reduction of protein *O*-mannosyltransferases in *Drosophila melanogaster* resulted in defects in embryonic muscle development [16–19] and *POMT1* deletion in mouse resulted in embryonic death [20]. Protein *O*-mannosyltransferases in *Saccharomyces cerevisiae* (ScPmtps) are composed of at least six members (Scpmtp1–6) that form hetero- and homo-complexes in various combinations [21,22]. ScPmtp1 has been proposed to consist of seven transmembrane helices [23]. The ScPmtp1 N-terminus and loops 2, 4 and 6 are located in the cytoplasm, and the C-terminus and loops 1, 3 and 5 are located in the ER lumen. Two hydrophilic regions (loops 5 and 1) are important for enzymatic activity [21,23,24]. We recently constructed models in which human POMT1 and POMT2 have seven- and nine-transmembrane helices respectively and in which the C-termini and loops 1, 3 and 5 are located in the ER lumen [25]. This is similar to the topology of ScPmtp1. In ScPmtp1, Arg^{64}, Glu^{78} and Arg^{138} have been shown to be essential for enzymatic activity [24].

Here, we investigated whether amino acids of human POMT1 and POMT2 corresponding to Arg^{64}, Glu^{78} and Arg^{138} in ScPmtp1 are required for transferase activity and complex formation.

2. Materials and methods

2.1. Vector construction of POMT1 and POMT2 mutants

Human POMT1 cDNA was used for site-directed mutagenesis and was cloned into pcDNA 3.1/Zeocin (−) (Invitrogen Corp.,

* Corresponding author. Fax: +81 3 3579 4776.
E-mail address: endo@tmig.or.jp (T. Endo).

0006-291X/$ - see front matter © 2011 Elsevier Inc. All rights reserved.
doi:10.1016/j.bbrc.2011.07.012

Carlsbad, CA), and human POMT2 cDNA was cloned into pcDNA 3.1/Hygromycin (+) as described previously [1,2]. For each of the mutations (R30A, E44A, R105A /R72A, E86A, R145A) examined in this study, the *POMT1* and *POMT2* gene was modified with a QuickChange Site-Directed Mutagenesis Kit (STRATAGENE, La Jolla, CA) according to the manufacturer's instructions. The mutants were generated with following primer pairs: R30A, 5′-ATGGGGTTA CTGAGCGCGCTGTGGCGACTCACC-3′ and 5′-GGTGAGTCGCCACAGC GCGCTCAGTAACCCCAT-3′; E44A, 5′-CGCGGGCTGTGGTTTTTGACGC AGTATATTATG-3′ and 5′-CATAATATACTGCGTCAAAAACCACAGCCC GCG-3′; R105A 5′-CCTGTGTGGTCCCTGGCCCTGCTGCCAGCACTC-3′ and 5′-GAGTGCTGGCAGCAGGGCCAGGACCACACAGG-3′; R72A, 5′-CTGTCCTTCGCCACCGCCTTCCACCGCTTGGACG-3′ and 5′-CGTCCAA GCGGTGGAAGGCGGTGGCGAAGGACAG-3′; E86A, 5′-CCGCACATC TGTTGGGATGCGACTCACTTTGGAAAAATG-3′ and 5′-CATTTTTCCAA AGTGAGTCGCATCCCAACAGATGTGCGG-3′; R145A, 5′-CAGCTACAT GGGAATGGCAGGATTCTGTGCATTCCTTGGC -3′ and 5′-GCCAAGGA ATGCACAGAATCCTGCCATTCCCATGTAGCTG-3′. All mutant clones were sequenced to confirm the presence of the mutations.

2.2. Cell culture and expression of POMT mutants

Human embryonic kidney (HEK) 293T cells were maintained in Dulbecco's modified Eagle's medium (Invitrogen) supplemented with 10% fetal bovine serum, 2 mM L-glutamine, 100 units/ml penicillin and 50 mg/ml streptomycin at 37 °C with 5% CO_2. Expression plasmids were transfected into HEK293T cells using Lipofectamine Plus reagent (Invitrogen) according to the manufacturer's instructions. Cells were incubated for 3 days to produce POMT1 and POMT2 proteins. The cells were homogenized in 10 mM Tris–HCl, pH 7.4, 1 mM EDTA, 250 mM sucrose, 1 mM DTT, with protease inhibitor mixture (3 mg/ml pepstatin A, 1 mg/ml leupeptin, 1 mM benzamidine-HCl, 1 mM PMSF). After centrifugation at 900×*g* for 10 min, the supernatant was subjected to ultracentrifugation at 100,000×*g* for 1 h. The precipitate was used as the microsomal fraction. Protein concentration was determined by BCA assay (Thermo Fisher Scientific Inc., Waltham, MA, USA). Microsomal fractions were solubilized with 20 mM Tris–HCl, pH 8.0, 2 mM 2-mercaptoethanol, 10 mM EDTA and 0.5% *n*-octyl-β-D-thioglucoside at 4 °C. After centrifugation at 10,000×*g* for 10 min, the supernatant was used as solubilized supernatant.

2.3. Western blot analysis

The microsomal fractions (20 μg) were separated by SDS–PAGE (7.5% gel) and proteins were transferred to a PVDF membrane. The membrane was blocked in PBS containing 5% skim milk and 0.05% Tween 20, incubated with anti-POMT2 polyclonal antibody [2] or anti-myc (A-14) antibody (Santa Cruz Biotechnology Inc., Santa Cruz, CA), and treated with anti-rabbit IgG conjugated with horseradish peroxidase (HRP) or anti-mouse IgG conjugated with HRP (GE Healthcare Bio-sciences Corp., Piscataway, NJ). Proteins that bound to the antibody were visualized with an ECL kit (GE Healthcare Bio-sciences). As reported previously [1,2], anti-POMT1 and anti-POMT2 polyclonal antibodies did not detect endogenous POMT1 and POMT2, respectively. Each antibody is specific for the respective recombinant protein. That is, they do not cross-react with each other.

2.4. Assay for POMT activity

POMT activity was based on the amount of mannose transferred from Dol-P-Man to a glutathione-S-transferase fusion α-DG (GST-α-DG) as described previously with a slight modification [1]. Briefly, assays were carried out in a 20 μl reaction volume containing 20 mM Tris–HCl (pH 8.0), 100 nM [^{3}H]-labeled Dol-P-Man (Dol-P-[^{3}H]Man, 125,000 dpm/pmol, American Radiolabeled Chemicals, St. Louis, MO), 2 mM 2-mercaptoethanol, 10 mM EDTA, 0.5% *n*-octyl-β-D-thioglucoside, 10 μg of GST-α-DG, and 80 μg of microsomal membrane fraction. Microsomal fractions were solubilized with buffer containing 20 mM Tris–HCl (pH 8.0), 2 mM 2-mercaptoethanol, 10 mM EDTA, 0.5% *n*-octyl-β-D-thioglucoside for 1 h and the reaction was initiated by adding Dol-P-[^{3}H]Man. After 1 h incubation at 25 °C, the reaction was stopped by adding 150 μl of PBS containing 1% Triton X-100, and the reaction mixture was centrifuged at 10,000×*g* for 10 min. The supernatant was removed, mixed with 400 μl of PBS containing 1% Triton X-100 and 10 μl of Glutathione-Sepharose 4B beads (GE Healthcare Bio-sciences), rotated at 4 °C for 1 h, and washed three times with 20 mM Tris–HCl (pH 7.4) containing 0.5% Triton X-100. The radioactivity adsorbed to the beads was measured with a liquid scintillation counter. POMT activities were normalized by protein expression levels.

2.5. Immunoprecipitation

Microsomal fractions were lysed with assay buffer (20 mM Tris–HCl, pH 8.0, 2 mM 2-mercaptoethanol, 10 mM EDTA, 0.5% *n*-octyl-β-D-thioglucoside) in a final concentration of 2 mg/ml for 5 h at 4 °C. After solubilization, proteins were subjected to centrifugation at 10,000×*g* for 30 min and pre-cleaned with CL-6B Sepharose (Sigma–Aldrich, St. Louis, MO). Pre-cleaned supernatants were mixed with anti-myc (9E10) agarose conjugate (Santa Cruz Biotech) and incubated overnight. After 3 washes with the assay buffer, the agarose beads were suspended in sample buffer. Samples were subjected to Western blot analysis.

3. Results and discussion

In the present study, we attempted to elucidate the importance of three amino acids in the enzymatic activity and complex formation of human POMTs. Previously, Arg^{64}, Glu^{78} and Arg^{138} in ScPmt1p were reported to be critical for enzymatic activity [24]. In particular, Arg^{138} is essential for complex formation with ScPmt2p [24]. The membrane topologies of human POMT1 (Fig. 1A) and POMT2 (Fig. 1B) were predicted from bioinformatics analyses [25]. The corresponding three amino acids are conserved in human POMT1 and POMT2 (Fig. 1C). Therefore, we substituted Arg^{30}, Glu^{44} and Arg^{105} in human POMT1 and Arg^{72}, Glu^{86} and Arg^{145} in human POMT2 with Ala by site-direct mutagenesis and expressed the genes in HEK293T cells with their wild-type partners.

Western blots showed that both the POMT1 mutants (Fig. 2A) and the POMT2 mutants (Fig. 3A) were expressed normally, and their mobilities in SDS–PAGE were not affected by the amino acid substitutions. All mutated POMT1s and POMT2s were co-precipitated with wild-type POMT2 or wild-type POMT1, respectively (Figs. 2B and 3B). Each protein expression level of transfectants and the amount of proteins in the immunoprecipitates were determined densitometrically. Low precipitation of R145A-mutant (Fig. 3B) seems to be due to low expression level of protein (Fig. 3A). The expression ratio of R145A-POMT2/POMT1 was about 60% of wild-type POMT2/POMT1. The precipitated ratio of R145A-POMT2/POMT1 was about 70% of wild-type POMT2/POMT1. The expressed POMT2/POMT1 ratios of other mutants were around 80% to 120% and precipitated POMT2/POMT1 ratios were comparable to those of wild-type POMT2/POMT1. Taken together, three amino acids substituted in human POMT1 and POMT2 are not essential for POMT1–POMT2 complex formation. In ScPmt1p, Arg^{138} is essential for complex formation with ScPmt2p [24]. Therefore, changing this residue to Ala caused loss

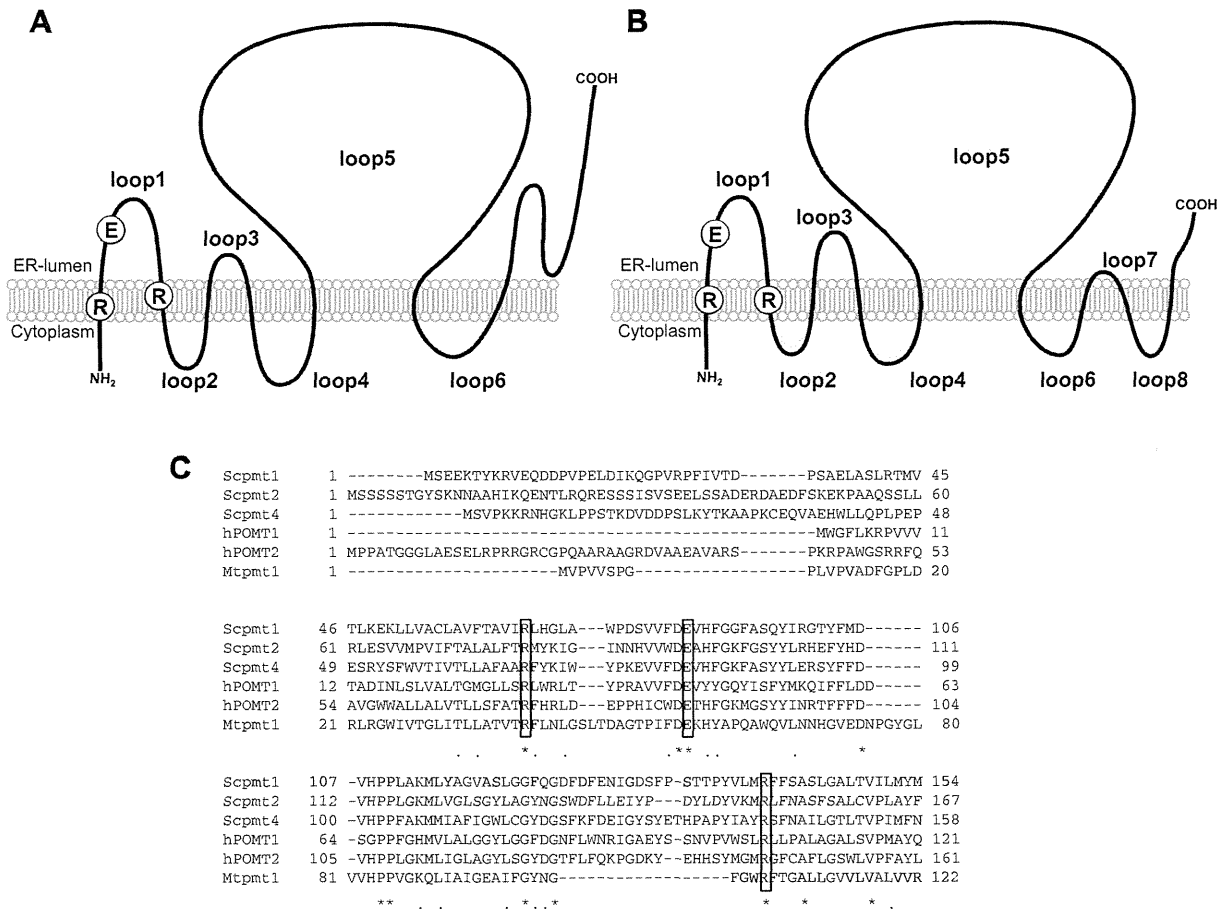

Fig. 1. Schematic representation of human POMT1 and POMT2, and alignment of PMT family members. (A) and (B), Topology models of human POMT1 and POMT2 according to [25]. R, E and R indicate the sites where Arg, Glu and Arg were substituted with Ala by site-directed mutagenesis. The major splicing variant of human POMT1, which lacks amino acids 234–255, was used in this study [2]. (C), ClustalW alignment of *N*-terminal amino acid sequences of protein *O*-mannosyltransferases. ScPmt, *S. cerevisiae* Pmt; hPOMT, human POMT; Mtpmt, *M. tuberculosis* pmt. Dots indicate similar amino acids. Asterisks indicate conserved amino acids. Squares indicate amino acids substituted to Ala.

of enzymatic activity. However, in human POMT1, the same amino acid substitution did not affect POMT1–POMT2 complex formation. These results suggest that Arg^{138} of ScPmt1p and Arg^{105} of human POMT1 have different roles. A phylogenetic analysis showed that the PMT family has three subfamilies: PMT1, PMT2, and PMT4 [12]. ScPmt1p and ScPmt2p are members of the PMT1 and PMT2 subfamilies, respectively. On the other hand, human POMT1 and POMT2 are members of the PMT4 and PMT2 subfamilies, respectively. The members of the PMT1 subfamily form complexes with members of the PMT2 subfamily, and a single member of the PMT4 subfamily (ScPmt4p) forms a homomeric complex and does not form a complex with ScPmt2p [21]. Although *S. cerevisiae* has at least six PMT family members, humans have only two PMT members, POMT1 and POMT2. Therefore, POMT1 and POMT2 must form a heterodimeric complex to have mannosyl transfer activity. This may explain why Arg^{138} of ScPmt1p and Arg^{105} of human POMT1 have different roles.

Next, we examined the effect of amino acid substitution on protein *O*-mannosyltransferase activity. Each of the substitutions in human POMT1 abolished most of the activity (Fig. 2C), indicating that Arg^{30}, Glu^{44} and Arg^{105} in loop1 of POMT1 are essential for POMT activity. On the other hand, the POMT2 mutants retained enzymatic activities (Fig. 3C). R72A-mutant and E86A-mutant sustained about 65% and 75% activity of wild-type POMT, respectively, and R145A-mutant retained enzymatic activity entirely. These results clearly show that these three amino acids play different roles in POMT1 and POMT2.

It is not clear why human protein *O*-mannosyltransferase activity requires co-expression of two components, POMT1 and POMT2 [1,2]. One possibility is that assembly of POMT1 and POMT2 creates a catalytic domain but each POMT1 or POMT2 itself does not have any catalytic activity. Another possibility is that POMT1 or POMT2 is a catalytic molecule and another component may enhance its activity. Recently, we found that zebra fish POMT2 alone expressed in HEK293T cells showed weak activity, while zebra fish POMT1 alone showed no activity [26], suggesting that zebra fish POMT2 itself has enzymatic activity, or may form a complex with endogenous POMT1 resulting in low levels of enzymatic activity. In addition, dermal fibroblast cells from WWS patients with mutations in *POMT1* showed low residual activity [10,12], suggesting that POMT2 has low levels of activity without POMT1. Taken together, these findings indicate that human POMT1 and POMT2 are required for efficient mannose transfer, although they are probably not functionally equivalent.

It is not clear whether loops 1 of ScPmt2p and ScPmt1p have similar roles. Although the substitutions in loop 1 of human POMT2 had little effect on transferase activity (Fig. 3C), POMT activity of lymphoblasts of a WWS patient homozygous for a Tyr96Cys mutation in loop 1 of POMT2 was extremely low [9]. This